



Research article

Stability and bifurcation analysis in predator-prey system involving Holling type-II functional response

Jocirei D. Ferreira^{1,*}, Wilmer L. Molina², Jhon J. Perez² and Aida P. González²

¹ Institute of Exact and Earth Science, Federal University of Mato Grosso, Barra do Garças-MT, Brazil

² Department of Mathematics, University of Cauca, Popayán, Colombia

* **Correspondence:** Email: jocireiufmt@gmail.com; Tel: +55-66-9-9216-3907; Fax: +556634021110.

Abstract: In this article, we focused on the study of codimension-one Hopf bifurcations and the associated Lyapunov stability coefficients in the context of general two-dimensional reaction-diffusion systems defined on a finite fixed-length segment. Algebraic expressions for the first Lyapunov coefficients are provided for the infinite-dimensional system subject to Neumann boundary conditions. As an application, a diffusive predator-prey system modeling competing populations with a Holling type-II functional response for the predator was analyzed and studied under Neumann boundary conditions. Our main goal is to perform a detailed, local stability analysis of the proposed model, showing the existence of multiple spatially homogeneous and non-homogeneous periodic orbits, arising from the occurrence of a codimension-one Hopf bifurcation.

Keywords: reaction-diffusion system; Lyapunov coefficients; predator-prey system; spatially homogeneous bifurcation; spatially non-homogeneous bifurcation; finite-length segment

1. Introduction

Dynamic models describing interactions between populations whether competitive, cooperative, or predator-prey are fundamental tools in mathematical ecology. They play a crucial role in understanding, predicting, and managing biological systems in both natural and engineered environments. In microbiology, these models shed light on key interactions such as bacterial competition, virus-host dynamics, and microbial predation, which are central to understanding infection spread, community assembly, and antibiotic resistance. By analyzing how population parameters and their variations affect species development, these models help describe, predict, regulate, and control evolutionary dynamics.

The origins of these models trace back to the early 20th century, notably to the independent work of Lotka (1925) and Volterra (1926), who introduced a system of differential equations to capture predator-prey dynamics. The Lotka-Volterra framework has since been widely adapted in microbial systems to study phenomena such as bacteriophage predation on bacteria, competition between antibiotic-sensitive and resistant strains, and interactions within microbial communities in biofilms or the human gut. Over time, many extensions of the classical Lotka-Volterra model have been developed to incorporate ecological complexities like carrying capacity, functional responses, and time delays (see [1–3]). In particular, reaction-diffusion models have become essential for studying how spatial heterogeneity and movement affect population dynamics. Studies [3] have shown how spatial interactions and environmental feedbacks can generate complex behaviors such as pattern formation, spatial chaos, and spatiotemporal oscillations. For microorganisms, reaction-diffusion models have been used to investigate bacterial colony expansion, the effects of antibiotic gradients, and the diffusion of quorum-sensing molecules regulating collective behaviors.

The classical Lotka-Volterra model aims to quantify intra- and interspecific interactions and their relationship with the environment by examining the temporal evolution of populations. However, time and space are inseparable in ecological systems. A comprehensive understanding of population dynamics requires accounting for spatial variation in predator and prey densities. Classical models often assume uniform population densities, a simplification rarely met in nature. In reality, populations are spatially heterogeneous, and both predators and prey adapt their movement and survival strategies in response to this variability. These spatial differences result in diffusion processes that generate population movement patterns, profoundly influencing ecosystem dynamics. Incorporating diffusion into predator-prey models is thus both more realistic and essential to capturing the full range of population behaviors observed in nature. Mathematically, this leads to reaction-diffusion systems, which combine local reactions (birth, death, predation) with spatial movement. In microbiology, diffusion is central to the transport of nutrients, signaling molecules, antibiotics, and viruses, shaping competition, cooperation, and the emergence of resistance. Diffusion describes the displacement of individuals across a medium, from molecules and bacteria to larger organisms, and even collective phenomena like epidemics or rumor spread. This movement occurs within a spatial domain Ω , typically an open subset of \mathbb{R}^n , with $n \geq 1$. Diffusion arises in nonliving particles, like molecules in solution, and in living organisms, whose movements are often driven by resource seeking or predator avoidance. The resulting spatial patterns reveal the influence of diffusive processes, as seen in examples like insect tunnels, snail trails, fungal fairy rings, mussel bed patterns, animal coat markings, and leaf arrangements. In microorganisms, striking patterns include bacterial swarms, fungal colony rings, and the heterogeneity of biofilms or microbial mats.

Population growth depends not only on reproduction or predation but also on spatial movement. Simple models without mobility assume equal interaction probability regardless of location, useful in confined systems like small lakes or laboratory environments. However, most ecosystems involve movement across larger, variable territories, affecting reproduction, foraging, and survival. Models that account for spatial distribution and movement in one, two, or three dimensions are therefore more realistic for example, fish in the ocean, animals on the savannah, or insects in vegetation. In microbial systems, such models explain infection spread across tissues, microbial colony expansion on agar, and the spatial organization of consortia in environments like soil, wastewater, or the human microbiome.

Because all species live in spatial environments, their movement is key to growth and distribution.

A fundamental ecological principle is that organisms tend to move from high-density to low-density regions, promoting expansion and reducing resource competition. Consequently, spatial models are increasingly used to analyze predator-prey interactions. Migration and dispersal often expose organisms to survival challenges, and predator pressure drives prey to relocate to safer areas. Predators, in turn, adapt by tracking prey movements. Mobility thus shapes both individual survival and long-term population dynamics. For detailed discussions on spatial effects, see [4, 5]. In microorganisms, mobility includes bacterial chemotaxis, phage diffusion, and plasmid transfer processes critical for survival under environmental stress, infection propagation, and horizontal gene transfer.

In this paper, we study the effect of diffusion on predator-prey dynamics, focusing on a codimension-one Hopf bifurcation with environmental carrying capacity as the bifurcation parameter. Our main contribution is to derive an explicit formula for the first Lyapunov coefficient, which determines the direction and stability of emerging periodic solutions. Biologically, this predicts whether small oscillations near equilibrium will amplify (leading to persistent cycles) or decay (leading to stable coexistence). This has practical importance, for example, in understanding whether systems like lynx-hare or pest-natural enemy populations stabilize or cycle. Our analysis clarifies the role of space and movement in generating oscillatory patterns and provides a concrete criterion for predicting qualitative behavior near the bifurcation point.

To address the need for models incorporating both temporal and spatial variation, we begin by outlining Hopf bifurcation methods for general reaction-diffusion systems. We apply this framework to a predator-prey system with two predator species and one prey species, deriving the first Lyapunov coefficient as a function of system parameters, with particular attention to carrying capacity. Biologically, including two predator species captures interspecific competition and niche differentiation, while the carrying capacity reflects environmental support for the prey population, indirectly influencing predator persistence. Our results offer insights into how environmental constraints and predator interactions shape ecosystem dynamics, with potential applications in biodiversity conservation and pest management. This coefficient is key to identifying whether the Hopf bifurcation is supercritical or subcritical and assessing the stability of the resulting periodic solutions.

It is worth noting that a related analysis was conducted in [6] for n -dimensional ordinary differential equation (ODE) systems, where expressions for the first four Lyapunov coefficients were derived. Following this approach, we review the method proposed in [7] (see also [8, 9]) to compute the first Lyapunov coefficient in nonlinear autonomous reaction-diffusion systems. With minor modifications, this method can be extended to calculate higher-order Lyapunov coefficients; for details on the second coefficient, see [9]. Finally, similar analyses can be performed on domains $\Omega \subset \mathbb{R}^N$ ($N = 1, 2, 3$), which is relevant for studying how dimensionality affects reaction-diffusion models. Ecologically, extending to higher dimensions enables the modeling of realistic habitats with complex topography or fragmented landscapes, improving our understanding of how spatial structure influences biodiversity and population persistence. We leave this analysis for future work, as it lies beyond the scope of this paper.

As an application of the Hopf bifurcation formula, we analyze the occurrence of a codimension-1 Hopf bifurcation in a predator-prey interaction model with diffusion, which constitutes a restricted version of a reaction-diffusion model for competing populations, represented by the following system

of partial differential equations (PDEs):

$$\begin{aligned} u_t &= d_1 u_{xx} + \gamma u \left(1 - \frac{u}{K}\right) - m_1 \frac{u}{a_1 + u} v - m_2 \frac{u}{a_2 + u} w, & x \in \Omega, t > 0, \\ v_t &= d_2 v_{xx} + m_1 \frac{u}{a_1 + u} v - \beta_1 v, & x \in \Omega, t > 0, \\ w_t &= d_3 w_{xx} + m_2 \frac{u}{a_2 + u} w - \beta_2 w, & x \in \Omega, t > 0. \end{aligned} \quad (1.1)$$

We assume that the functions u , v , and w satisfy the following Neumann boundary conditions and initial conditions:

$$\begin{aligned} u_x(0, t) &= v_x(0, t) = w_x(0, t) = 0 & t > 0, \\ u_x(\ell, t) &= v_x(\ell, t) = w_x(\ell, t) = 0 & t > 0, \\ u(x, 0) &= u_0(x), v(x, 0) = v_0(x), w(x, 0) = w_0(x) & x \in \Omega, \end{aligned} \quad (1.2)$$

where $\Omega = (0, \ell\pi)$ is an open connected bounded interval of \mathbb{R} with $\ell \in \mathbb{R}^+$; $u = u(x, t)$ is the population density of the prey, and $v = v(x, t)$, $w = w(x, t)$ are the population densities of two predators competing for the prey; $d_1, d_2, d_3 > 0$ are the diffusion rates; γ is the intrinsic rate of increase of the prey; K represents the carrying capacity of the environment that depends on the state x , with respect to the prey; $m_i > 0$, $\beta_i > 0$, and $a_i > 0$ are the maximum birth rate, the death rate, and the half saturation constant, respectively, of the i th predator ($i = 1, 2$). We assume that the functional response function $f_i(u) = \frac{u}{a_i + u}$, for $i = 1, 2$, and $0 < a_2 < a_1$, is Holling type II for each predator. A logistic growth of the prey is assumed if no predator is present. We are particularly interested in studying the stability of isolated equilibrium populations, where we assume that the prey and predators are diffusing in the domain $\Omega = (0, \ell\pi)$, although our calculations can be carried over to higher spatial domains. To ensure that the equilibrium of systems (1.1)–(1.2) corresponds to that of the related ODE model, we consider Neumann boundary conditions, which preserve the spatially homogeneous steady states. Other studies on this type of model can be found in [10–13].

It is worth noting that a detailed bifurcation analysis for the ODE version of models (1.1)–(1.2), which describes the temporal variation of two predator species competing for a single prey, was given in [14] (see also [15]). Subsequently, a class of models that describes this competition is proposed and analyzed in the literature (see for example [16–18]). The ODE dynamics of systems (1.1)–(1.2) describes the competition of an “ r -strategist” and a “ k -strategist” for a single regenerating prey species. We note that an r -strategist is a species that tries to ensure its survival by having a relatively high growth rate and a k -strategist is a species that consumes less, has a lower growth rate, and can raise its offsprings on a scarce supply of food. In the following, we present a very brief summary of some results obtained in [14] for the system

$$\begin{aligned} \dot{u} &= \gamma u \left(1 - \frac{u}{K}\right) - m_1 \frac{u}{a_1 + u} v - m_2 \frac{u}{a_2 + u} w, & t > 0, \\ \dot{v} &= m_1 \frac{u}{a_1 + u} v - \beta_1 v, & t > 0, \\ \dot{w} &= m_2 \frac{u}{a_2 + u} w - \beta_2 w, & t > 0, \end{aligned} \quad (1.3)$$

where the parameters appearing in system (1.3) have the same meaning as those appearing in system (1.1). The equilibria of (1.3) are

$$(u, v, w) = (0, 0, 0), \quad (u, v, w) = (K, 0, 0),$$

and the points on the straight line segment

$$L_K = \left\{ (u, v, w) \in \mathbb{R}^3 : u = \lambda^*, v \geq 0, w \geq 0 \text{ and } m_1 \frac{v}{a_1 + \lambda^*} + m_2 \frac{w}{a_2 + \lambda^*} = \gamma \left(1 - \frac{\lambda^*}{K}\right) \right\}, \quad (1.4)$$

in the positive octant of the (u, v, w) -space, provided we assume that

$$m_1 > \beta_1, m_2 > \beta_2, \text{ and } \lambda^* = \frac{a_1 \beta_1}{m_1 - \beta_1} = \frac{a_2 \beta_2}{m_2 - \beta_2}. \quad (1.5)$$

It is easy to see that the eigenvalues of the Jacobian matrix at the equilibrium point $(0, 0, 0)$ are γ , $-\beta_1$ and $-\beta_2$, which implies that the equilibrium point $(0, 0, 0)$ is unstable. On the other hand, since $0 < \lambda^* < K$ and the eigenvalues of the Jacobian matrix at the equilibrium point $(K, 0, 0)$ are $-\gamma < 0$, $\frac{m_1 K}{a_1 + K} - \beta_1 > 0$, and $\frac{m_2 K}{a_2 + K} - \beta_2 > 0$, it follows that the equilibrium point $(K, 0, 0)$ is also unstable. It is clear that all equilibria on L_K are stable for all K that satisfy the inequality $\lambda^* < K \leq a_2 + 2\lambda^*$. This means that if food is scarce, both the r and k -strategists may live together in the long run in a steady state that depends on the initial values of the species. When $a_2 + 2\lambda^* < K < a_1 + 2\lambda^*$ (considering $a_1 > a_2$) the family of equilibria on the line L_K undergoes a split, and part of L_K becomes unstable; that is, there exists a point $(\lambda^*, \xi_1(K), \xi_2(K))$ on L_K such that the equilibria on

$$L_U = \{(\lambda^*, \xi_1, \xi_2) \in L_K : \xi_1 < \xi_1(K)\},$$

are unstable for the flow of (1.3), and the equilibria on

$$L_S = \{(\lambda^*, \xi_1, \xi_2) \in L_K : \xi_1 > \xi_1(K)\},$$

are stable.

The point $(\xi_1(K), \xi_2(K))$ is obtained solving the system

$$\begin{aligned} \frac{m_1 \xi_1}{a_1 + \lambda^*} + \frac{m_2 \xi_2}{a_2 + \lambda^*} &= \frac{\gamma(K - \lambda^*)}{K}, \\ \frac{m_1 \xi_1}{(a_1 + \lambda^*)^2} + \frac{m_2 \xi_2}{(a_2 + \lambda^*)^2} &= \frac{\gamma}{K}. \end{aligned} \quad (1.6)$$

As K takes on the value $a_1 + 2\lambda^*$, the equilibrium that exists in the (u, v) -plane is stable, while all other equilibria on L_K lose stability. When $K > a_1 + 2\lambda^*$, all equilibria on L_K become unstable. Note that as K increases from $a_2 + 2\lambda^*$ to $a_1 + 2\lambda^*$, the point $(\lambda^*, \xi_1(K), \xi_2(K))$ moves along L_K continuously from $(\lambda^*, 0, \xi_2(K))$ to $(\lambda^*, \xi_1(K), 0)$, so that the points left behind become unstable. From the point of view of the competition, as the quantity of available food increases, the k -strategist loses ground, and those equilibria where the relative growth of the k -strategist is high compared to the growth of the r -strategist are the first to be destabilized. When K reaches the value $a_1 + 2\lambda^*$, all interior equilibria become destabilized, and the only stable equilibrium remaining is the endpoint of L in the (u, v) -plane. This means that, at this value of the carrying capacity, the k -strategist dies out. One may prove that if K is increased further, then even the equilibrium in the (u, v) -plane gets destabilized, but the prey and the r -strategist continue to coexist in a periodic manner due to the occurrence of an Andronov-Hopf bifurcation (see [14], Theorem 3.3, pp. 1304).

The main purpose of this exposition is to extend the result stated in Theorem 3.3 of [14] for the reaction-diffusion systems (1.1)–(1.2), considering its restriction to the u, v or u, w planes. In other words, we demonstrate that the prey and one of the predators (either the r -strategist or k -strategist) can

continue to coexist periodically due to the occurrence of an Andronov-Hopf bifurcation, even when diffusion is included in system (1.3). Although several researchers have addressed the spatial version of systems (1.3) [16,17,19], to the best of our knowledge, no results have been reported in the literature that examine the direction of the Hopf bifurcation and the stability of the emerging periodic solutions for the restriction of system (1.1)–(1.2).

Following the bifurcation analysis carried out in Theorem 3.3 of [14] for the restriction of the system (1.3), we conduct a detailed bifurcation study of the constant coexistence equilibrium solution of systems (1.1)–(1.2), when restricted to the invariant planes u, v or u, w of \mathbb{R}^3 , within the spatial domain $\Omega = (0, \ell\pi)$, with $\ell \in \mathbb{R}^+$. We show that, under certain parameter conditions, the restriction of systems (1.1)–(1.2) to these invariant planes undergoes a codimension-1 Hopf bifurcation. Additionally, the resulting periodic orbits can be either spatially homogeneous, coinciding with the periodic solution of the corresponding system of ordinary differential equations, or spatially non-homogeneous, leading to temporal oscillations or non-constant stationary patterns. Furthermore, we demonstrate that there exist exactly n Hopf bifurcation points where spatially non-homogeneous periodic orbits emerge. These periodic orbits correspond to the spatial eigenmodes $\frac{\cos(jx)}{\ell}$ ($1 \leq j \leq n$), where $\ell\pi$ represents the length of the spatial domain. The integer n depends on ℓ and increases as ℓ grows.

Although the analysis for the restriction of systems (1.1)–(1.2) to the invariant planes u, v or u, w of \mathbb{R}^3 resembles that in the literature [8], we highlight that, in this paper, we consider the restriction of a deterministic competition model among two populations of microorganisms (the predators populations) for a single nutrient (the prey population), in a chemostat with constant input rate. The chemostat is a laboratory apparatus used for the continuous culture of microorganisms. It is interesting to note that competition in predator-prey models differs from that of competition in microbial populations, more popularly known as chemostat models. These models can be used to study the competition between populations of microorganisms for a growth-limiting substrate, and have the advantage that certain biological parameters presumed to influence competitive outcome can be controlled by the experiment. Evidently, in the case of predator-prey models, the predators have to put effort in securing prey, while in microbes the predator is not required to put in effort as they grow in cultured medium, and the nutrients reach the microbes. For this reason, though competition occurs in microbes, the study yields different dynamics. The ecological environment created by a chemostat is one of the few controlled experimental systems for testing microbial growth and competition. As a tool in biotechnology, the chemostat plays an important role in bioprocessing. The basic phenomenon is modeled and analyzed using the dynamical systems approach. Accordingly, our purpose of this work is to demonstrate that the prey (considered the nutrient) and one of the predators (considered the microorganisms: Either the r -strategist or k -strategist) may coexist periodically due to the occurrence of an Andronov-Hopf bifurcation, even when diffusion is included in system (1.3).

Finally, it is worth observing that predator-prey models presenting Hopf bifurcation and considering diffusion, as the model analyzed in this article, are a powerful tool to study complex biological dynamics, such as those observed in pathology, immunology, and antimicrobial resistance. Our model can be adapted to problems of tumor pathology, immunology, infections, and antimicrobial resistance, where the prey can be considered tumor cells, pathogenic bacteria, and sensitive and resistant bacterial populations, and predators as immune cells (T or NK lymphocytes), macrophages or antibiotics and antimicrobials or phagocytes, respectively. In these cases, Hopf

oscillations reflect the alternation between tumor growth and immune response, representing changes in bacterial load and immune activation (as in recurrent sepsis) and dynamics of resistance emergence and collapse of the sensitive population. On the other hand, the diffusion in each case simulates tumor invasion into surrounding tissue and models the spread of infection through tissues or the flow of immune cells and the movement of resistant bacteria in heterogeneous environments. Accordingly, a predator-prey model that integrates Hopf bifurcation and diffusion can provide a solid basis for understanding the complex dynamics of diseases and the interaction between pathogens and defense systems, opening doors for more effective and personalized treatments.

This paper is organized as follows. In Section 2, we present a review of the method found in [7] (see also [8]) for the calculation of the first Lyapunov coefficient for a general reaction-diffusion system. In Section 3, we investigate the invariant regions for systems (1.1)–(1.2). Furthermore, considering the restriction of systems (1.1)–(1.2) either to the u , v or u , w invariant planes of \mathbb{R}^3 , we defer a study of its homogeneous equilibrium points (or homogeneous solutions) and investigate their asymptotic behavior. Finally, as an application of the Hopf bifurcation formula, we consider the related codimension 1 Hopf bifurcation for the restricted system with the spatial domain $\Omega = (0, \ell\pi)$, $\ell \in \mathbb{R}^+$. Specifically, we show the occurrence of spatially homogeneous and non-homogeneous codimension 1 Hopf bifurcation for the restriction of systems (1.1)–(1.2) either to the u , v or u , w planes of \mathbb{R}^3 . A discussion follows in the final section.

2. Outline of the Hopf bifurcation method for a class of reaction diffusion systems

In this section, we provide an overview of the method outlined in [7] (see also [8, 9]) for computing the first Lyapunov coefficient in a general reaction-diffusion system with Neumann boundary conditions. Notably, the expression for the first Lyapunov coefficient, denoted as l_1 , plays a crucial role in analyzing the codimension-1 Hopf bifurcation in a class of reaction-diffusion systems subject to Neumann boundary conditions.

Accordingly, we consider the reaction diffusion model represented by the following PDE system

$$\begin{aligned} u_t &= d_1 \Delta u + f(u, v, K), & x \in \Omega, t > 0, \\ v_t &= d_2 \Delta v + g(u, v, K), & x \in \Omega, t > 0, \end{aligned} \quad (2.1)$$

subject to Neumann boundary conditions

$$\frac{\partial u}{\partial \nu}(x, t) = \frac{\partial v}{\partial \nu}(x, t) = 0 \quad \text{on} \quad \partial\Omega \times (0, \infty), \quad (2.2)$$

and initial conditions

$$u(x, 0) = u_0(x), \quad v(x, 0) = v_0(x) \quad \text{on} \quad \Omega. \quad (2.3)$$

Here, $\Omega \subset \mathbb{R}^N$ ($N \geq 1$), $\nu = \vec{\nu}(x)$ denotes the outer unit normal to $\partial\Omega$, $\Delta = \sum_{j=1}^N \partial^2 / \partial x_j^2$ is the Laplacian operator, $d_i > 0$, $i = 1, 2$ are the diffusion rates, and $K \in \mathbb{R}^+$ is a parameter. As a starting point in this exposition, we consider a one dimensional domain $\Omega = (0, \ell\pi)$ with $\ell \in \mathbb{R}^+$; the functions $f, g : \mathbb{R} \times \mathbb{R}^2 \rightarrow \mathbb{R}$ are C^k ($k \geq 5$) with $f(0, 0, K) = g(0, 0, K) = 0$. We define the real-valued Sobolev space

$$\chi := \{(u, v) \in H^2(0, \pi\ell) \times H^2(0, \pi\ell) : (u_x, v_x)|_{x=0, \pi\ell} = 0\},$$

and its complexification

$$\chi_{\mathbb{C}} := \chi \oplus i\chi = \{x_1 + ix_2 : x_1, x_2 \in \chi\}.$$

If we consider the Taylor expansion of the functions f and g at $(0, 0, K)$, where K is the bifurcation parameter, the linearized system associated with (2.1)–(2.3) at $(0, 0, K)$ is given by

$$\begin{pmatrix} u_t \\ v_t \end{pmatrix} = L(K) \begin{pmatrix} u \\ v \end{pmatrix}, \quad \text{where } L(K) = \begin{pmatrix} d_1 \frac{\partial^2}{\partial x^2} + A(K) & B(K) \\ C(K) & d_2 \frac{\partial^2}{\partial x^2} + D(K) \end{pmatrix},$$

is the linearized operator with domain $D_{L(K)} = \chi_{\mathbb{C}}$ and

$$A(K) = f_u(0, 0, K); B(K) = f_v(0, 0, K); C(K) = g_u(0, 0, K); D(K) = g_v(0, 0, K).$$

Thus, to study the occurrence of Hopf bifurcation, systems (2.1)–(2.3) must satisfy the following hypothesis:

Hopf hypothesis: There exists a neighborhood $B(K_0, \delta)$ of K_0 such that for $K \in B(K_0, \delta)$, $L(K)$ has a pair of complex, simple, conjugate eigenvalues $\beta(K) = \alpha(K) \pm i\omega(K)$, continuously differentiable in K , such that $\alpha(K_0) = 0$, $\omega(K_0) = \omega_0 > 0$, and $\alpha'(K_0) \neq 0$. Furthermore, all other eigenvalues of $L(K)$ have no null real parts for $K \in B(K_0, \delta) - \{K_0\}$.

Hence, to perform the Hopf bifurcation analysis of systems (2.1)–(2.3), we analyze the eigenvalues of the differential operator $L(K)$. This analysis starts by considering the Sturm-Liouville problem in its basic form, which serves as a fundamental tool for reducing the dimensionality of the system and enables efficient theoretical and numerical investigation.

$$\begin{aligned} -\varphi'' &= \mu\varphi, & x &\in (0, \ell\pi), \\ \varphi'(0) &= \varphi'(\ell\pi) = 0. \end{aligned}$$

has eigenvalues $\mu_n = \frac{n^2}{\ell^2}$, $n = 0, 1, 2, 3, \dots$, with corresponding eigenfunctions $\varphi_n(x) = \cos\left(\frac{nx}{\ell}\right)$. Let

$$\begin{pmatrix} \psi \\ \phi \end{pmatrix} = \sum_{n=0}^{\infty} \cos \frac{nx}{\ell} \begin{pmatrix} a_n \\ b_n \end{pmatrix}, \quad (2.4)$$

be an eigenfunction of $L(K)$ with eigenvalue $\beta(K)$, that is $L(K)(\psi, \phi)^T = \beta(K)(\psi, \phi)^T$. The following proposition follows immediately by taking into account (2.4) and, therefore, the proof is omitted.

Proposition 1. For each $n = 0, 1, 2, 3, \dots$ we have that $\begin{pmatrix} a_n \\ b_n \end{pmatrix}$ is an eigenvector of the operator $L_n(K)$ defined by

$$L_n(K) = \begin{pmatrix} A(K) - \frac{d_1 n^2}{\ell^2} & B(K) \\ C(K) & D(K) - \frac{d_2 n^2}{\ell^2} \end{pmatrix},$$

with eigenvalue $\beta(K)$, that is

$$L_n(K) \begin{pmatrix} a_n \\ b_n \end{pmatrix} = \beta(K) \begin{pmatrix} a_n \\ b_n \end{pmatrix}, \quad n = 0, 1, 2, 3, \dots,$$

where a_n and b_n are the Fourier coefficients of ψ and ϕ , respectively.

Proposition 1 states that the eigenvalues of $L(K)$ are given by the eigenvalues of $L_n(K)$ for $n = 0, 1, 2, \dots$. Therefore, we consider the characteristic equation of $L_n(K)$, which is given by

$$\beta^2 - T_n(K)\beta + D_n(K) = 0, \quad n = 0, 1, 2, \dots,$$

where

$$T_n(K) = \left[\left(A(K) - \frac{d_1 n^2}{\ell^2} \right) + \left(D(K) - \frac{d_2 n^2}{\ell^2} \right) \right] \quad \text{and} \quad D_n(K) = \left(A(K) - \frac{d_1 n^2}{\ell^2} \right) \left(D(K) - \frac{d_2 n^2}{\ell^2} \right) - B(K)C(K),$$

and the eigenvalues $\beta(K)$ are given by

$$\beta(K) = \frac{T_n(K) \pm \sqrt{T_n^2(K) - 4D_n(K)}}{2}, \quad n = 0, 1, 2, \dots \quad (2.5)$$

Following the framework of [7] (see also [8]), we can write system (2.1) in the abstract form

$$\frac{dU}{dt} = L(K)U + F(K, U), \quad (2.6)$$

where

$$F(K, U) = \begin{pmatrix} f(u, v, K) - A(K)u - B(K)v \\ g(u, v, K) - C(K)u - D(K)v \end{pmatrix},$$

with $U = (u, v)^T \in \chi$. In particular, at $K = K_0$, system (2.6) takes the form

$$\frac{dU}{dt} = L(K_0)U + F_0(U) \quad \text{where} \quad F_0(U) = F(K_0, U).$$

We introduce on $\chi_{\mathbb{C}}$ the complex-valued $L^2(0, \ell\pi)$ inner product defined by

$$\langle U_1, U_2 \rangle = \int_0^{\ell\pi} (\bar{u}_1 u_2 + \bar{v}_1 v_2) dx,$$

with $U_i = (u_i, v_i)^T \in \chi_{\mathbb{C}}$ ($i = 1, 2$), where $\langle \lambda U_1, U_2 \rangle = \bar{\lambda} \langle U_1, U_2 \rangle$. We denote by $L^*(K_0)$ to the adjoint operator $L(K_0)$, which satisfies $\langle U, L(K_0)V \rangle = \langle L^*(K_0)U, V \rangle$ for all $U, V \in \chi_{\mathbb{C}}$ with $D_{L^*(K_0)} = \chi_{\mathbb{C}}$. Consequently, the adjoint operator of $L(K_0)$ is given by

$$L^*(K_0) = \begin{pmatrix} d_1 \frac{\partial^2}{\partial x^2} + A(K_0) & C(K_0) \\ B(K_0) & d_2 \frac{\partial^2}{\partial x^2} + D(K_0) \end{pmatrix}.$$

As in Proposition 1, it can be proved that $(a_n^*, b_n^*)^T$ is an eigenvector of $L_n^*(K_0)$, $n = 1, 2, 3, \dots$, with eigenvalue $\bar{\beta}(K_0)$, where

$$L_n^*(K_0) := \begin{pmatrix} A(K_0) - \frac{d_1 n^2}{\ell^2} & C(K_0) \\ B(K_0) & D(K_0) - \frac{d_2 n^2}{\ell^2} \end{pmatrix}.$$

If the Hopf hypothesis holds at $K = K_0$, then $L(K_0)$ has a pair of simple purely imaginary eigenvalues $\pm i\omega_0$ if and only if there exists a unique $n \in \mathbb{N}$ such that $\pm i\omega_0$ are purely imaginary eigenvalues of $L_n(K_0)$. We denote the associated eigenvector by $q = \cos \frac{nx}{\ell}(a_n, b_n)^T$, with $a_n, b_n \in \mathbb{C}$, such that $L(K_0)q = i\omega_0 q$. Furthermore, we can choose $q^* = \cos \frac{nx}{\ell}(a_n^*, b_n^*)^T \in \chi_{\mathbb{C}}$ as an eigenfunction of $L^*(K_0)$, such that

$$L^*(K_0)q^* = -i\omega_0 q^*, \quad \langle q^*, \bar{q} \rangle = 0 \quad \text{and} \quad \langle q^*, q \rangle = 1.$$

We introduce the spaces

$$\chi^c := \{zq + \bar{z}\bar{q} : z \in \mathbb{C}\} \quad \text{and} \quad \chi^{su} := \{u \in \chi : \langle q^*, u \rangle = 0\}.$$

Proposition 2. *Let χ^c be the generalized eigenspace of $L(K_0)$ corresponding to the eigenvalues with null real parts and χ^{su} the space of functions $u \in \chi$ such that $\langle q^*, u \rangle = 0$. The space χ can be decomposed as $\chi = \chi^c \oplus \chi^{su}$.*

Proof. The proof of this proposition is found in [9]. □

From proposition 2, if $U = (u, v)^T \in \chi$, there exists $r = (r_1, r_2)^T \in \chi^{su}$ and $z \in \mathbb{C}$ such that

$$\begin{pmatrix} u \\ v \end{pmatrix} = zq + \bar{z}\bar{q} + \begin{pmatrix} r_1 \\ r_2 \end{pmatrix} \quad \text{or} \quad \begin{cases} u = za_n \cos \frac{nx}{\ell} + \bar{z}\bar{a}_n \cos \frac{nx}{\ell} + r_1, \\ v = zb_n \cos \frac{nx}{\ell} + \bar{z}\bar{b}_n \cos \frac{nx}{\ell} + r_2. \end{cases} \quad (2.7)$$

Proposition 3. *In coordinate (2.7), the variables z and r can be expressed as*

$$\begin{aligned} z &= \langle q^*, U \rangle, \\ r &= U - \langle q^*, U \rangle q - \langle \bar{q}^*, U \rangle \bar{q}. \end{aligned} \quad (2.8)$$

Furthermore, in coordinate (2.8), system (2.6) assumes the form

$$\begin{aligned} \frac{dz}{dt} &= i\omega_0 z + \langle q^*, F_0(U) \rangle, \\ \frac{dr}{dt} &= L(K_0)r + H(z, \bar{z}, r), \end{aligned} \quad (2.9)$$

where

$$H(z, \bar{z}, r) = F_0(U) - \langle q^*, F_0(U) \rangle q - \langle \bar{q}^*, F_0(U) \rangle \bar{q} \quad \text{and} \quad F_0 = F_0(zq + \bar{z}\bar{q} + r). \quad (2.10)$$

Proof. The proof of this proposition is found in [9]. □

Following [7], $F_0(U) = F(K_0, U)$ can be written as

$$F_0(U) = \frac{1}{2}\mathbf{B}(U, U) + \frac{1}{6}\mathbf{C}(U, U, U) + o(\|U\|^4), \quad (2.11)$$

where $\mathbf{B}_{XY} = \mathbf{B}(X, Y)$, $\mathbf{C}_{XYZ} = \mathbf{C}(X, Y, Z)$, are symmetric *multilinear* functions with $X = (x_1, x_2)^T$, $Y = (y_1, y_2)^T$.

In coordinates, we have

$$B_i(X, Y) = \sum_{j,k=1}^3 \left[\frac{\partial^2 F_i(K_0, \eta)}{\partial \eta_j \partial \eta_k} \right]_{\eta=0} x_j y_k \quad \text{and} \quad C_i(X, Y, Z) = \sum_{j,k,l=1}^3 \left[\frac{\partial^3 F_i(K_0, \eta)}{\partial \eta_j \partial \eta_k \partial \eta_l} \right]_{\eta=0} x_j y_k z_l,$$

to then calculate, for later uses,

$$\mathbf{B}(q, q) = \mathbf{B}_{qq} = \cos^2 \frac{nx}{\ell} \begin{pmatrix} c_n \\ d_n \end{pmatrix}; \quad \mathbf{B}(q, \bar{q}) = \mathbf{B}_{q\bar{q}} = \cos^2 \frac{nx}{\ell} \begin{pmatrix} e_n \\ f_n \end{pmatrix}; \quad \mathbf{C}(q, q, \bar{q}) = \mathbf{C}_{qq\bar{q}} = \cos^3 \frac{nx}{\ell} \begin{pmatrix} g_n \\ h_n \end{pmatrix},$$

where

$$\begin{aligned} c_n &= f_{uu} a_n^2 + 2f_{uv} a_n b_n + f_{vv} b_n^2, \\ d_n &= g_{uu} a_n^2 + 2g_{uv} a_n b_n + g_{vv} b_n^2, \\ e_n &= f_{uu} |a_n|^2 + f_{uv} (a_n \bar{b}_n + \bar{a}_n b_n) + f_{vv} |b_n|^2, \\ f_n &= g_{uu} |a_n|^2 + g_{uv} (a_n \bar{b}_n + \bar{a}_n b_n) + g_{vv} |b_n|^2, \\ g_n &= f_{uuu} |a_n|^2 a_n + f_{uuv} (2|a_n|^2 b_n + a_n^2 \bar{b}_n) + f_{uvv} (2|b_n|^2 a_n + b_n^2 \bar{a}_n) + f_{vvv} |b_n|^2 b_n, \\ h_n &= g_{uuu} |a_n|^2 a_n + g_{uuv} (2|a_n|^2 b_n + a_n^2 \bar{b}_n) + g_{uvv} (2|b_n|^2 a_n + b_n^2 \bar{a}_n) + g_{vvv} |b_n|^2 b_n. \end{aligned} \quad (2.12)$$

with all the partial derivatives evaluated in $(0, 0, K_0)$. From (2.10), (2.11) and given that

$$H(z, \bar{z}, r) = \frac{H_{20}}{2} z^2 + H_{11} z \bar{z} + \frac{H_{02}}{2} \bar{z}^2 + o(|z| |r|), \quad (2.13)$$

we have

$$\begin{aligned} H_{20} &= \mathbf{B}_{qq} - \langle q^*, \mathbf{B}_{qq} \rangle q - \langle \bar{q}^*, \mathbf{B}_{qq} \rangle \bar{q}; \quad H_{11} = \mathbf{B}_{q\bar{q}} - \langle q^*, \mathbf{B}_{q\bar{q}} \rangle q - \langle \bar{q}^*, \mathbf{B}_{q\bar{q}} \rangle \bar{q}; \\ H_{02} &= \mathbf{B}_{\bar{q}\bar{q}} - \langle q^*, \mathbf{B}_{\bar{q}\bar{q}} \rangle q - \langle \bar{q}^*, \mathbf{B}_{\bar{q}\bar{q}} \rangle \bar{q}. \end{aligned}$$

From Appendix A of [7], system (2.9) has a center manifold that can be represented locally as the graphic of a smooth function

$$W^c(0) = \{(z, \bar{z}, r) : r = V(z, \bar{z})\},$$

with $V : \mathbb{C}^2 \rightarrow X^{su}$. Thus, we can write r in the form

$$\begin{aligned} r &= V(z, \bar{z}) \\ &= \sum_{j+k=2} \frac{1}{j!k!} r_{jk} z^j \bar{z}^k + o(|z|^3) \\ &= \frac{r_{20}}{2} z^2 + r_{11} z \bar{z} + \frac{r_{02}}{2} \bar{z}^2 + o(|z|^3), \end{aligned}$$

with $\langle q^*, r_{ij} \rangle = 0$ and $r_{jk} = \bar{r}_{kj} \in \mathbb{C}^2$, $j+k=2$.

Proposition 4. From (2.10), (2.11), and (2.13), and observing that

$$\frac{dr}{dt} = \frac{\partial r}{\partial z} \frac{dz}{dt} + \frac{\partial r}{\partial \bar{z}} \frac{d\bar{z}}{dt} = L(K_0)r + H(z, \bar{z}, r),$$

we obtain

$$\begin{aligned} -[L(K_0) - 2i\omega_0 I] r_{20} &= \mathbf{B}_{qq} - \langle q^*, \mathbf{B}_{qq} \rangle q - \langle \bar{q}^*, \mathbf{B}_{qq} \rangle \bar{q}, \\ -L(K_0) r_{11} &= \mathbf{B}_{q\bar{q}} - \langle q^*, \mathbf{B}_{q\bar{q}} \rangle q - \langle \bar{q}^*, \mathbf{B}_{q\bar{q}} \rangle \bar{q}, \\ -[L(K_0) + 2i\omega_0 I] r_{02} &= \mathbf{B}_{\bar{q}\bar{q}} - \langle q^*, \mathbf{B}_{\bar{q}\bar{q}} \rangle q - \langle \bar{q}^*, \mathbf{B}_{\bar{q}\bar{q}} \rangle \bar{q}, \end{aligned}$$

Proof. The proof of this proposition is found in [9]. \square

It can be verified that $\int_0^{\ell\pi} \cos^3 \frac{nx}{\ell} dx = 0$ for all $n \in \mathbb{N}$ and, therefore

$$\langle q^*, \mathbf{B}_{qq} \rangle = \langle q^*, \mathbf{B}_{q\bar{q}} \rangle = \langle q^*, \mathbf{B}_{\bar{q}\bar{q}} \rangle = \langle \bar{q}^*, \mathbf{B}_{qq} \rangle = \langle \bar{q}^*, \mathbf{B}_{q\bar{q}} \rangle = \langle \bar{q}^*, \mathbf{B}_{\bar{q}\bar{q}} \rangle = 0.$$

Consequently,

$$\begin{aligned} r_{20} &= \begin{cases} -[L(K_0) - 2i\omega_0 I]^{-1} \mathbf{B}_{qq}, & \text{if } n \in \mathbb{N}, \\ -[L(K_0) - 2i\omega_0 I]^{-1} (\mathbf{B}_{qq} - \langle q^*, \mathbf{B}_{qq} \rangle q - \langle \bar{q}^*, \mathbf{B}_{qq} \rangle \bar{q}), & \text{if } n = 0, \end{cases} \\ &= \begin{cases} -[L(K_0) - 2i\omega_0 I]^{-1} \left[\left(\frac{1}{2} \cos \left(\frac{2nx}{\ell} \right) + \frac{1}{2} \right) \begin{pmatrix} c_n \\ d_n \end{pmatrix} \right], & \text{if } n \in \mathbb{N}, \\ -[L(K_0) - 2i\omega_0 I]^{-1} \left[\begin{pmatrix} c_0 \\ d_0 \end{pmatrix} - \langle q^*, \mathbf{B}_{qq} \rangle \begin{pmatrix} a_0 \\ b_0 \end{pmatrix} - \langle \bar{q}^*, \mathbf{B}_{qq} \rangle \begin{pmatrix} \bar{a}_0 \\ \bar{b}_0 \end{pmatrix} \right], & \text{if } n = 0. \end{cases} \end{aligned} \quad (2.14)$$

Likewise

$$\begin{aligned} r_{11} &= \begin{cases} -[L(K_0)]^{-1} \left[\left(\frac{1}{2} \cos \left(\frac{2nx}{\ell} \right) + \frac{1}{2} \right) \begin{pmatrix} e_n \\ f_n \end{pmatrix} \right], & \text{if } n \in \mathbb{N}, \\ -[L(K_0)]^{-1} \left[\begin{pmatrix} e_0 \\ f_0 \end{pmatrix} - \langle q^*, \mathbf{B}_{q\bar{q}} \rangle \begin{pmatrix} a_0 \\ b_0 \end{pmatrix} - \langle \bar{q}^*, \mathbf{B}_{q\bar{q}} \rangle \begin{pmatrix} \bar{a}_0 \\ \bar{b}_0 \end{pmatrix} \right], & \text{if } n = 0. \end{cases} \end{aligned} \quad (2.15)$$

It is worth observing that the calculation of $[2i\omega_0 I - L(K_0)]^{-1}$ and $[L(K_0)]^{-1}$ in (2.14) and (2.15) are restricted to the subspaces spanned by the eigen-modes 1 and $\cos(\frac{2nx}{\ell})$.

Consequently, the reaction–diffusion system (2.9) restricted to the center manifold is given by

$$\frac{dz}{dt} = i\omega_0 z + \langle q^*, F_0(\mathbf{V}(z, \bar{z})) \rangle = i\omega_0 z + \sum_{2 \leq i+j \leq 3} \frac{g_{ij}}{i!j!} z^i \bar{z}^j + O(|z|^4),$$

where

$$g_{20} = \langle q^*, \mathbf{B}_{qq} \rangle; g_{11} = \langle q^*, \mathbf{B}_{q\bar{q}} \rangle; g_{02} = \langle q^*, \mathbf{B}_{\bar{q}\bar{q}} \rangle \text{ and } g_{21} = 2 \langle q^*, \mathbf{B}_{r_{11}q} \rangle + \langle q^*, \mathbf{B}_{r_{20}\bar{q}} \rangle + \langle q^*, \mathbf{C}_{qq\bar{q}} \rangle \quad (2.16)$$

Therefore, the Poincaré normal form of (2.6) for K in a neighborhood of K_0 can be written in the form

$$\frac{dz}{dt} = (\alpha + i\omega)z + z \sum_{j=1}^M c_j(K) (z\bar{z})^j,$$

where $\alpha + i\omega = \alpha(K) + i\omega(K)$, z is a complex variable, $M \geq 1$ and $c_j(K)$ are complex-valued coefficients (see [7, 9]). The value $c_1(K_0)$ is given by

$$c_1(K_0) = \frac{i}{2\omega_0} \left(g_{20}g_{11} - 2|g_{11}|^2 - \frac{1}{3}|g_{02}|^2 \right) + \frac{g_{21}}{2}. \quad (2.17)$$

Definition 1. The first Lyapunov coefficient is defined by

$$l_1(K_0) = \frac{\operatorname{Re}(c_1(K_0))}{\omega_0} = \frac{1}{\omega_0} \operatorname{Re} \left(\frac{i}{2\omega_0} \left(g_{20}g_{11} - 2|g_{11}|^2 - \frac{1}{3}|g_{02}|^2 \right) + \frac{1}{2}g_{21} \right), \quad (2.18)$$

with g_{20} , g_{11} , g_{02} , and g_{21} given by (2.16).

Taking into account the Hopf hypothesis, from Theorem II and Remark 3 in chapter 1 of [7], system (2.6) exhibits Hopf bifurcation in $K = K_0$. Furthermore, for $K = K(s)$ with s sufficiently small, there exists a family of $T(s)$ -periodic continuously differentiable solutions $(u(s)(x, t), v(s)(x, t), K(s))$, such that $u(0) = v(0) = 0$, where

$$\begin{aligned} u(s)(x, t) &= s \left(a_n e^{\frac{2\pi i t}{T(s)}} + \bar{a}_n e^{\frac{-2\pi i t}{T(s)}} \right) \cos \frac{n}{\ell} x + o(s^2), \\ v(s)(x, t) &= s \left(b_n e^{\frac{2\pi i t}{T(s)}} + \bar{b}_n e^{\frac{-2\pi i t}{T(s)}} \right) \cos \frac{n}{\ell} x + o(s^2), \end{aligned} \quad (2.19)$$

with

$$\begin{aligned} T(s) &= \frac{2\pi}{\omega_0} \sum_{i=0}^M \tau^{(i)}(0) s^i + o(s^{M+1}); \quad \tau(0) = 1; \quad \tau'(0) = 0; \\ \tau''(0) &= \frac{-1}{\omega_0} \left[\operatorname{Im}(c_1(K_0)) - \frac{\operatorname{Re}(c_1(K_0))}{\alpha'(K_0)} \omega'(K_0) \right]; \end{aligned}$$

$\tau'''(0) = 0$, and $\alpha'(K_0) \neq 0$ is the transversality condition.

We have the following theorem.

Theorem 1. Assume that Hopf Hypothesis is satisfied. Then, system (2.6) undergoes a Hopf bifurcation, that is, it has a family of real-valued $T(s)$ -periodic solutions $(u(s)(x, t), v(s)(x, t), K(s))$ for s sufficiently small bifurcating from $(0, 0, K_0) \in \chi \times \mathbb{R}$, and there exists a unique $n \in \mathbb{N}_0$ such that $(u(s)(x, t), v(s)(x, t))$ can be parameterized in the form of (2.19). Furthermore:

1) The Hopf bifurcation is supercritical if

$$\frac{1}{\alpha'(K_0)} \operatorname{Re}(c_1(K_0)) < 0;$$

2) The Hopf bifurcation is subcritical if

$$\frac{1}{\alpha'(K_0)} \operatorname{Re}(c_1(K_0)) > 0,$$

where $\alpha'(K_0)$ is the derivative of the real part of the eigenvalue of $L(K)$ at $K = K_0$.

3) If the other eigenvalues of $L(K_0)$ have real part negative, then the bifurcation of the periodic solutions is stable if $\operatorname{Re}(c_1(K_0)) < 0$ and unstable if $\operatorname{Re}(c_1(K_0)) > 0$.

3. Stability and bifurcation analysis for the restriction of systems (1.1)–(1.2)

As a start point of this section, we observe that the first quadrant is an invariant region for the restriction of systems (1.1)–(1.2) to the u, v plane. Next, we discuss the homogeneous solutions and investigate their asymptotic behavior. For sake of completeness, we study the persistence and permanence properties, and the global attractor for the solutions of the restricted system. Finally, we consider the related codimension 1 Hopf bifurcation with the spatial domain $\Omega = (0, \ell\pi)$, $\ell \in \mathbb{R}^+$. We point out that all the analysis carried out in this section is analogous for the restriction of systems (1.1)–(1.2) to the u, w plane and is omitted.

3.1. Equilibria and stability analysis

We now consider the restriction of the systems (1.1)–(1.2) to the plane u, v . For sake of simplicity, from now on, we drop the index of the variables and parameters composing systems (1.1)–(1.2), despite the diffusion rates; we also rename β_1, m_1, a_1 as d, m, a , respectively. Accordingly, the restricted system to be studied is represented by the following PDE model

$$\begin{aligned} u_t &= d_1 u_{xx} + \gamma u \left(1 - \frac{u}{K}\right) - m \frac{u}{a+u} v, & x \in \Omega, t > 0, \\ v_t &= d_2 v_{xx} + m \frac{u}{a+u} v - dv, & x \in \Omega, t > 0, \end{aligned} \quad (3.1)$$

with Neumann boundary conditions and initial conditions

$$\begin{aligned} u_x(0, t) = v_x(0, t) = 0, \quad u_x(\pi\ell, t) = v_x(\pi\ell, t) = 0, & \quad t > 0, \\ u(x, 0) = u_0(x), \quad v(x, 0) = v_0(x), & \quad x \in \Omega. \end{aligned} \quad (3.2)$$

Here, $\Omega = (0, \ell\pi)$ is an open connected bounded interval of \mathbb{R} with $\ell \in \mathbb{R}^+$.

Proposition 5. *The region $\Sigma = \{(u, v) : u \geq 0, v \geq 0\}$ is invariant for systems (3.1)–(3.2)*

Proof. This is immediate from [20], Theorem 14.11 pp. 203. \square

In the following, we discuss the homogeneous solutions of systems (3.1)–(3.2), that is, the solutions of the system

$$\begin{aligned} \gamma \left(1 - \frac{u}{K}\right) u - m \frac{u}{a+u} v &= 0, & t > 0, \\ m \frac{u}{a+u} v - dv &= 0, & t > 0. \end{aligned} \quad (3.3)$$

Let $\lambda = \frac{ad}{m-d}$ be the prey *quantity threshold* for the predator species. Then, aside from the solutions $(u_0, v_0) = (0, 0)$ and $(u_1, v_1) = (K, 0)$, system (3.3) has biologically interesting solutions only if $m > d$ and $K > \lambda$. We observe that the predator species may survive only if $0 < \lambda < K$, the latter condition implying $m > d$ too. Throughout this paper, we assume that the inequality $0 < \lambda < K$ holds. Thus, the homogeneous solutions of systems (3.1)–(3.2) are the origin $(u_0, v_0) = (0, 0)$, the point $(u_1, v_1) = (K, 0)$, and the point $(u_2, v_2) = \left(\lambda, \frac{\gamma(K-\lambda)(a+\lambda)}{Km}\right)$.

To study the qualitative behavior of these homogeneous solutions, observe that the linearization of system (3.1) at a critical point (u^*, v^*) is given by

$$\begin{aligned} u_t &= d_1 \Delta u + \left(\gamma \left(1 - \frac{u^*}{K}\right) - \frac{\gamma u^*}{K} - \frac{m a v^*}{(a + u^*)^2} \right) u - \frac{m u^*}{a + u^*} v, & x \in \Omega, t > 0, \\ v_t &= d_2 \Delta v + \frac{m a v^*}{(a + u^*)^2} u + \left(\frac{m u^*}{a + u^*} - d \right) v, & x \in \Omega, t > 0, \end{aligned} \quad (3.4)$$

with boundary and initial conditions given by (3.2).

Let $0 = \mu_0 < \mu_1 < \mu_2 < \dots \rightarrow \infty$ and $\{\psi_n\}_{n=0}^\infty$ be the eigenvalues and eigenfunctions of the Laplacian operator in Ω with Neumann boundary on $\partial\Omega$:

$$\begin{aligned} -\Delta \psi_n &= \mu_n \psi_n & \text{in } \Omega, \\ \frac{\partial \psi_n}{\partial \nu} &= 0 & \text{on } \partial\Omega. \end{aligned} \quad (3.5)$$

We can assume that $\{\psi_n\}_{n=0}^\infty$ is an orthonormal basis of $L^2(\Omega)$.

Let $\phi = (u, v)$, $D = \text{diag}(d_1, d_2)$, and J be the matrix

$$J(u^*, v^*) = \begin{pmatrix} \gamma \left(1 - \frac{u^*}{K}\right) - \frac{\gamma u^*}{K} - \frac{ma v^*}{(a+u^*)^2} & -\frac{mu^*}{a+u^*} \\ \frac{mav^*}{(a+u^*)^2} & \frac{mu^*}{a+u^*} - d \end{pmatrix}.$$

Then, (3.4) can be written as

$$\frac{\partial \phi}{\partial t} = D\Delta \phi + J\phi.$$

Thus, the solution of (3.4), (3.2) with initial condition $\phi(\cdot, 0) = \phi_0$, is given by

$$\phi(x, t) = \sum_{n=0}^{\infty} e^{(J - \mu_n D)t} \langle \phi_0, \psi_n \rangle \psi_n(x), \quad (3.6)$$

where $\langle \phi_0, \psi_n \rangle = \int_{\Omega} \phi_0(x) \psi_n(x) dx$.

It follows from the linearization principle that a homogeneous solution of (3.1)–(3.2) is locally asymptotically stable if the eigenvalues of all matrices $J - \mu_n D$ have negative real parts. If there exists an n such that $J - \mu_n D$ has an eigenvalue with positive real part, then the solution is unstable.

Remark 1. Note that if (u^*, v^*) is an unstable equilibrium for the flow of the corresponding ODE system of system (3.1)–(3.2) then (u^*, v^*) is also an unstable homogeneous equilibrium for the flow of (3.1)–(3.2), since the subspace of the function independent of x is invariant for the flow of (3.1)–(3.2).

Proposition 6. The homogeneous equilibrium $(u_0, v_0) = (0, 0)$ of systems (3.1)–(3.2) is unstable. On the other hand, the homogeneous equilibrium $(u_1, v_1) = (K, 0)$ of systems (3.1)–(3.2) is unstable if $0 < \lambda < K$; it is locally asymptotically stable if $0 < K < \lambda$.

Proof. The instability of the equilibrium $(u_0, v_0) = (0, 0)$ at $\mu_0 = 0$ follows from the fact that matrix $J(0, 0)$ has two eigenvalues: One $\gamma > 0$ and other $-d < 0$. On the other hand, for $\mu_0 = 0$, $(u_1, v_1) = (K, 0)$ and $0 < \lambda < K$, $J(K, 0)$ has a positive eigenvalue, which implies the instability of $(K, 0)$; if $0 < K < \lambda$ a straightforward calculation shows that the equilibrium $(K, 0)$ is stable according to Theorem 1.7 given in [21], since the eigenvalues of all matrix $J - \mu_n D$, $n = 0, 1, 2, \dots$, have negative real parts. \square

In the following, we study the local stability of $E = (u_2, v_2) = \left(\lambda, \frac{\gamma(K-\lambda)(a+\lambda)}{Km}\right)$, which is of biological interest if

$$0 < \lambda < K. \quad (3.7)$$

To study the local stability of equilibrium E , we assume condition (3.7) from now on. The Jacobian matrix J evaluated at E is given by

$$J(E) = \begin{pmatrix} \gamma \left(1 - \frac{\lambda}{K}\right) - \frac{\gamma \lambda}{K} - \frac{\gamma a(K-\lambda)}{K(a+\lambda)} & -\frac{m\lambda}{a+\lambda} \\ \frac{\gamma a(K-\lambda)}{K(a+\lambda)} & \frac{m\lambda}{a+\lambda} - d \end{pmatrix}.$$

Observing that $\frac{m\lambda}{a+\lambda} - d = 0$, we obtain

$$J(E) = \begin{pmatrix} -\frac{\gamma\lambda}{K} + \frac{\gamma\lambda(K-\lambda)}{K(a+\lambda)} & -\frac{m\lambda}{a+\lambda} \\ \frac{\gamma a(K-\lambda)}{K(a+\lambda)} & 0 \end{pmatrix}.$$

Proposition 7. *If $\lambda < K < a + 2\lambda$, the homogeneous equilibrium $E = \left(\lambda, \frac{\gamma(K-\lambda)(a+\lambda)}{Km}\right)$ of systems (3.1)–(3.2) is locally asymptotically stable. If $K > a + 2\lambda$, then E is unstable.*

Proof. The characteristic polynomial associated with $J(E) - \mu_n D$ is given by

$$J(E) - \mu_n D = \begin{pmatrix} -\frac{\gamma\lambda}{K} + \frac{\gamma\lambda(K-\lambda)}{K(a+\lambda)} - d_1\mu_n & -\frac{m\lambda}{a+\lambda} \\ \frac{\gamma a(K-\lambda)}{K(a+\lambda)} & -d_2\mu_n \end{pmatrix}.$$

$$p(\xi) = \xi^2 + \left[(d_1 + d_2)\mu_n + \frac{\gamma\lambda}{k} - \frac{\gamma\lambda(K-\lambda)}{K(a+\lambda)} \right] \xi + \mu_n d_2 \left(\mu_n d_1 + \frac{\gamma\lambda}{K} - \frac{\gamma\lambda(K-\lambda)}{K(a+\lambda)} \right) + \frac{m\lambda\gamma a(K-\lambda)}{K(a+\lambda)^2}.$$

Since by hypothesis $K < a + 2\lambda$, then $(d_1 + d_2)\mu_n + \frac{\gamma\lambda}{K} - \frac{\gamma\lambda(K-\lambda)}{K(a+\lambda)} > 0$ for all $n \geq 0$. Hence, from Theorem 1.7 given in [21], the homogeneous solution E of (3.1)–(3.2) is locally asymptotically stable. On the other hand, if $K > a + 2\lambda$, a straightforward calculation shows that for $n = 0$, $J(E)$ has a positive eigenvalue and, therefore, E is unstable. \square

In theoretical ecology, positivity and boundedness of the system establishes the biological well behaved nature of the system. On the other hand, persistence and permanence are important in the sense that they describe long term behavior of the system. Due to many reasons, such as pollution, over predation, over exploitation, mismanagement of natural resources, several species become extinct, and many others are at the point of extinction. Accordingly, the concept of persistence, meaning the survival of species for a longer time, has drawn lot of attention (see [22–25]). Analytically, a system is said to be persistent if it persists for each population, that is, if $\liminf_{t \rightarrow \infty} x(t) > 0$ (stronger case) or $\limsup_{t \rightarrow \infty} x(t) > 0$ (weaker case) for each population $x(t)$ of the system. Geometrically, persistence means that trajectories that initiate in a positive cone are eventually bounded away from coordinate planes. Later, one assures the survival of species in a biological sense.

For sake of completeness, we study the global attractor and persistence property for the solutions of systems (3.1)–(3.2). We show that the region $R = [0, K] \times [0, (\frac{\gamma}{d} + 1)K|\Omega|]$, where $|\Omega| = \int_{\Omega} dx$, is a global attractor that attracts all time-dependent solutions of the systems (3.1)–(3.2), regardless of initial functions. Finally, we note that the positive constant solution E of systems (3.1)–(3.2) is globally asymptotically stable under certain hypotheses. The next two propositions can be proved by the slight modifications of Theorems 2.1 and 2.2 given in [19] and the proof is omitted.

Proposition 8. *The non-negative solution (u, v) of the systems (3.1)–(3.2) satisfies $\limsup_{t \rightarrow \infty} u(t, x) \leq K$ and $\limsup_{t \rightarrow \infty} v(t, x) \leq (\frac{\gamma}{d} + 1)K|\Omega|$ on $\bar{\Omega}$.*

Proposition 9. The positive solution (u, v) of systems (3.1)–(3.2) satisfies $\liminf_{t \rightarrow \infty} u(t, x) \geq \delta$ and $\liminf_{t \rightarrow \infty} v(t, x) \geq \delta$ on $\bar{\Omega}$, for some sufficiently small $\delta > 0$, provided $\frac{d}{m} < \frac{K}{a+K}$.

Remark 2. In view of Proposition 8, we conclude the boundedness of the solutions of systems (3.1)–(3.2) and consequently, the system under consideration is dissipative. Therefore, any solution is defined for $t \geq 0$ and eventually enter the attracting compact set $R = [0, K] \times [0, (\frac{\gamma}{d} + 1)K|\Omega|]$, which implies that R is positive invariant. Hence, the system is dissipative, and its global attractor is contained in R . In theoretical ecology, positivity and boundedness of the system establishes the biological well behaved nature of the system. On the other hand, Proposition 9 ensures that systems (3.1)–(3.2) is persistent, provided that $\frac{d}{m} < \frac{K}{a+K}$. Persistence is important in the sense that it describes a long term behavior of the system. Accordingly, the concept of persistence means the survival of species for longer.

Proposition 10. If $0 < \lambda < K \leq a + \lambda$, then the positive constant solution E of systems (3.1)–(3.2) is globally asymptotically stable.

Proof. The result can be obtained by the slight modification of Theorem 2.5 given in [19]. For a positive solution $(u(t, x), v(t, x))$, we define the functional

$$W(t) = \int_{\Omega} V(u, v) dx \quad \text{where} \quad V(u, v) = \int_{u^*}^u \frac{\frac{s}{a+s} - \frac{u^*}{a+u^*}}{\frac{s}{a+s}} ds + \int_{v^*}^v \frac{r - v^*}{r} dr.$$

Thus, we have

$$\begin{aligned} W'(t) &= \int_{\Omega} \left(\frac{\frac{u}{a+u} - \frac{u^*}{a+u^*}}{\frac{u}{a+u}} d_1 \Delta u + \frac{v - v^*}{v} d_2 \Delta v \right) dx + \int_{\Omega} \left[V_u \left(\gamma \left(1 - \frac{u}{K} \right) u - \frac{mu}{a+u} v \right) + V_v \left(\frac{mu}{a+u} - d \right) v \right] dx \\ &= -\frac{ad_1 u^*}{a+u^*} \int_{\Omega} \frac{|\nabla u|^2}{u^2} dx - d_2 v^* \int_{\Omega} \frac{|\nabla v|^2}{v^2} dx + \int_{\Omega} \left[\left(\frac{mu}{a+u} - \frac{mu^*}{a+u^*} \right) \left(\frac{\gamma(1-\frac{u}{K})u}{\frac{mu}{a+u}} - v \right) + (v - v^*) \left(\frac{mu}{a+u} - d \right) \right] dx. \end{aligned} \quad (3.8)$$

Since $0 = \gamma(1 - \frac{u^*}{K})u^* - \frac{mu^*}{a+u^*}v^* = \frac{mu^*}{a+u^*} - d$, we have

$$\begin{aligned} W'(t) &= -\frac{ad_1 u^*}{a+u^*} \int_{\Omega} \frac{|\nabla u|^2}{u^2} dx - d_2 v^* \int_{\Omega} \frac{|\nabla v|^2}{v^2} dx \\ &\quad + \int_{\Omega} \left[\left(\frac{mu}{a+u} - \frac{mu^*}{a+u^*} \right) \left(\frac{\gamma(1-\frac{u}{K})u}{\frac{mu}{a+u}} - \frac{\gamma(1-\frac{u^*}{K})u^*}{\frac{mu^*}{a+u^*}} \right) \right] dx \\ &= -d_1 \frac{a\lambda}{a+\lambda} \int_{\Omega} \frac{|\nabla u|^2}{u^2} dx - d_2 \frac{\gamma(K-\lambda)(a+\lambda)}{Km} \int_{\Omega} \frac{|\nabla v|^2}{v^2} dx + \frac{ma}{a+\lambda} \int_{\Omega} \frac{(K-a-\lambda-u)(u-\lambda)^2}{a+u} dx < 0 : \forall t > 0 \end{aligned} \quad (3.9)$$

where, $u^* = \lambda$ and $v^* = \frac{\gamma(K-\lambda)(a+\lambda)}{Km}$. □

In the following, we concentrate on the investigation of codimension 1 Hopf bifurcation for systems (3.1)–(3.2).

3.2. Spatially homogeneous and non-homogeneous Hopf bifurcation for the constant coexistence steady state E

In this subsection, we focus on analyzing the codimension-1 Hopf bifurcation in the system (3.1)–(3.2), considering both spatially homogeneous and non-homogeneous cases.

Additionally, we determine the direction of the Hopf bifurcation and the stability of the emerging periodic solutions. It is worth noting that in [19], the authors examined the Hopf bifurcation in a class of reaction-diffusion predator-prey models, where the systems (3.1)–(3.2) was treated as a particular case. However, to the best of our knowledge, neither the direction of the Hopf bifurcation nor the stability of the bifurcating periodic solutions was studied. Therefore, our main goal in this subsection is to establish, through Hopf bifurcation, the emergence of periodic orbits in the restriction of systems (1.1)–(1.2) to the invariant u, v plane, as well as to determine the direction of the Hopf bifurcation and the stability of the resulting periodic solutions, following the analysis carried out in the ODE version of systems (1.1)–(1.2) (see [14] and other works such as [18, 26, 27]).

For the study of Hopf bifurcation, we take K as the bifurcation parameter and demonstrate that at $K = a + 2\lambda$, systems (3.1)–(3.2) undergoes a codimension-1 Hopf bifurcation. The resulting periodic orbits can be either spatially homogeneous, coinciding with the periodic solution of the associated ODE system, or spatially non-homogeneous. Furthermore, we establish that there exist exactly n Hopf bifurcation points where spatially non-homogeneous periodic orbits emerge. To structure our analysis according to the framework presented in Section 2, we shift the critical point $E = (\lambda, \frac{\gamma(K-\lambda)(a+\lambda)}{Km})$ of the systems (3.1)–(3.2) to the origin through a coordinate transformation

$$\begin{aligned}\hat{u} &= u - \lambda, \\ \hat{v} &= v - \frac{\gamma(K-\lambda)(a+\lambda)}{Km},\end{aligned}\tag{3.10}$$

and let u and v denote \hat{u} and \hat{v} , respectively. For the sake of simplicity, we denote $E = (\lambda, \xi_1)$, with $\xi_1 = \frac{\gamma(K-\lambda)(a+\lambda)}{Km}$, so that systems (3.1)–(3.2) takes the form

$$\begin{aligned}u_t - d_1 u_{xx} &= \gamma(u + \lambda) \left(1 - \frac{(u+\lambda)}{K}\right) - m \frac{(u+\lambda)(v+\xi_1)}{a+u+\lambda}, & x \in (0, \ell\pi), t > 0, \\ v_t - d_2 v_{xx} &= m \frac{(u+\lambda)(v+\xi_1)}{a+u+\lambda} - d(v + \xi_1), & x \in (0, \ell\pi), t > 0,\end{aligned}\tag{3.11}$$

satisfying the conditions

$$\begin{aligned}u_x(0, t) &= v_x(0, t) = 0, & t > 0, \\ u_x(\ell\pi, t) &= v_x(\ell\pi, t) = 0, & t > 0, \\ u(x, 0) &= u_0(x) - \lambda, \quad v(x, 0) = v_0(x) - \xi_1, & x \in (0, \ell\pi).\end{aligned}\tag{3.12}$$

Setting

$$f(u, v, K) = \gamma(u + \lambda) \left(1 - \frac{u + \lambda}{K}\right) - \frac{m(u + \lambda)(v + \xi_1)}{(a + u + \lambda)} \quad \text{and} \quad g(u, v, K) = \frac{m(u + \lambda)(v + \xi_1)}{(a + u + \lambda)} - d(v + \xi_1),$$

as in Section 2, we consider the linearization of systems (3.11)–(3.12) around the origin $E_0 = (0, 0)$

$$L(K) = \begin{pmatrix} d_1 \frac{\partial^2}{\partial x^2} + A(K) & B(K) \\ C(K) & d_2 \frac{\partial^2}{\partial x^2} + D(K) \end{pmatrix} \quad \text{and} \quad L_n(K) = \begin{pmatrix} A(K) - \frac{d_1 n^2}{\ell^2} & B(K) \\ C(K) & D(K) - \frac{d_2 n^2}{\ell^2} \end{pmatrix} \tag{3.13}$$

where

$$\begin{aligned}A(K) &= f_u(0, 0, K) = \frac{\gamma\lambda(K-a-2\lambda)}{K(a+\lambda)}, \quad B(K) = f_v(0, 0, K) = -d, \\ C(K) &= g_u(0, 0, K) = \frac{\gamma(K-\lambda)a}{K(a+\lambda)}, \quad D(K) = g_v(0, 0, K) = 0.\end{aligned}$$

The characteristic equation of $L_n(K)$ is given by

$$S^2 - T_n(K)S + D_n(K) = 0 \quad n = 0, 1, 2, 3, \dots, \quad (3.14)$$

where

$$T_n(K) = A(K) - \frac{(d_1+d_2)n^2}{\ell^2} = \frac{\gamma\lambda(K-a-2\lambda)}{K(a+\lambda)} - \frac{(d_1+d_2)n^2}{\ell^2} \quad \text{and} \quad D_n(K) = -\gamma\lambda \frac{(K-a-2\lambda)}{K(a+\lambda)} \frac{d_2 n^2}{\ell^2} + \frac{d_1 d_2 n^4}{\ell^4} + d \frac{\lambda(K-\lambda)a}{K(a+\lambda)}, \quad (3.15)$$

and $\alpha_n(K) \pm i\omega_n(K)$ are eigenvalues of L_n with $\alpha_n(K) = \frac{T_n(K)}{2}$ and $\omega_n(K) = \frac{1}{2} \sqrt{D_n(K) - \alpha_n^2(K)}$.

We identify the Hopf bifurcation value \bar{K} that satisfies the Hopf hypothesis that is, for which there exist a $n \in \mathbb{N} \cup \{0\}$, such that

$$T_n(K_0) = 0, \quad D_n(K_0) > 0, \quad \text{and} \quad T_j(K_0) \neq 0, \quad D_j(K_0) \neq 0 \quad \text{for} \quad j \neq n; \quad (3.16)$$

and for the unique pair of complex eigenvalues near the imaginary axis $\Gamma(K) = \alpha(K) \pm i\omega(K)$, we shall verify that $\alpha'(K_0) \neq 0$. Note that if $\lambda < K < a + 2\lambda$, we conclude from (3.15) that E_0 is locally asymptotically stable for systems (3.11)–(3.12). This local stability has already been established in Proposition 7 of Subsection 3.1. This suggests that any potential bifurcation point K_0 must be on the interval $[a + 2\lambda, \infty)$.

The next proposition shows that $K = K_0 = a + 2\lambda$ is the smallest bifurcation value at which E_0 (E) is a spatially homogeneous transversal Hopf point for systems (3.11)–(3.12) (for systems (3.1)–(3.2)), respectively.

Proposition 11. *At $K_0 = a + 2\lambda$ systems (3.11)–(3.12) satisfies the Hopf hypothesis. Consequently, E_0 is a transversal Hopf point for systems (3.11)–(3.12), which undergoes a Hopf bifurcation at K_0 .*

Proof. From (3.15), we obtain $\alpha_0(K_0) = 0$ and $\omega_0(K_0) = \sqrt{D_0(K_0)} > 0$. Therefore, $L_0(k_0)$ has a pair of pure imaginary eigenvalues. Furthermore, we conclude that $\alpha_n(K_0) < 0$ for all $n > 0$. Hence, all eigenvalues of $L_n(K_0)$, $n > 0$ has negative real part. Finally, a straightforward calculation gives $\frac{d}{dK} \alpha_n(K) > 0$ for all $n = 0, 1, 2, 3, \dots$ and $K \in [K_0, \infty)$, in particular for $K = K_0$. \square

Remark 3. *The result in Proposition 11 for $n = 0$ corresponds to the Hopf bifurcation of a spatially homogeneous periodic solution that is known from previous studies [14, 26]. Apparently, $K_0 = a + 2\lambda$ is also the unique value of K for the Hopf bifurcation of spatially homogeneous periodic solution for any $l > 0$.*

In the following, we concentrate on the study of the spatially non-homogeneous codimension 1 Hopf bifurcation for systems (3.11)–(3.12) for $n \geq 1$ that is, we identify the values of the bifurcation parameter K which satisfies the Hopf hypothesis. Thus we observe that the linearized operator of systems (3.11)–(3.12) evaluated at $E_0 = (0, 0)$ is given by (3.13), and the trace $T_n(K)$ and the determinant $D_n(K)$ are given in (3.15). As observed previously, any potential bifurcation point K must be on the interval $[a + 2\lambda, \infty)$.

For d_1, d_2, d , and λ fixed, we choose ℓ appropriately. Define

$$\ell_n = n \sqrt{\frac{d_1 + d_2}{M_*}}, \quad n \in \mathbb{N} \quad \text{where} \quad M_* = \frac{\gamma\lambda}{a + \lambda} > 0. \quad (3.17)$$

Then, for $\ell_n < \ell \leq \ell_{n+1}$ and $1 \leq j \leq n$, we define K_j as the roots of the equation

$$A(K) - \frac{(d_1 + d_2)j^2}{\ell^2} = 0 \text{ or equivalently } \frac{\gamma\lambda(K - a - 2\lambda)}{K(a + \lambda)} - \frac{(d_1 + d_2)j^2}{\ell^2} = 0. \quad (3.18)$$

These roots satisfy $K_0 < K_1 < K_2 < \dots < K_n$.

Remark 4. We observe that the roots K_j , $j = 1, 2, \dots, n$, indeed exist for $\ell_n < \ell \leq \ell_{n+1}$ and satisfies $K_0 < K_1 < K_2 < \dots < K_n$.

- Note that if $n = 1$ and $\ell_1 < \ell \leq \ell_2$, we have a unique bifurcation points K_1 , which is root of the equation $\frac{\gamma\lambda(K-a-2\lambda)}{K(a+\lambda)} - \frac{d_1+d_2}{\ell^2} = 0$ and given by $K_1 = \frac{\gamma\lambda\ell^2}{\gamma\lambda\ell^2 - (d_1+d_2)(a+\lambda)}(a+2\lambda)$. Note that $\gamma\lambda\ell^2 - (d_1 + d_2)(a + \lambda) > 0$ since $\ell_1 = \sqrt{\frac{d_1+d_2}{\frac{\gamma\lambda}{a+\lambda}}} < \ell$. Hence, $K_0 < K_1$.
- On the other hand, if $n = 2$ and $\ell_2 < \ell \leq \ell_3$, we have two bifurcation points, namely K_1 , which is root of the equation $\frac{\gamma\lambda(K-a-2\lambda)}{K(a+\lambda)} - \frac{(d_1+d_2)}{\ell^2} = 0$ and given by $K_1 = \frac{\gamma\lambda\ell^2(a+2\lambda)}{\gamma\lambda\ell^2 - (d_1+d_2)(a+\lambda)}$; and K_2 , which is root of the equation $\frac{\gamma\lambda(K-a-2\lambda)}{K(a+\lambda)} - \frac{(d_1+d_2)2^2}{\ell^2} = 0$ and given by $K_2 = \frac{\gamma\lambda\ell^2(a+2\lambda)}{\gamma\lambda\ell^2 - 4(d_1+d_2)(a+\lambda)}$. Note that $\gamma\lambda\ell^2 - (d_1 + d_2)(a + \lambda) > 0$ and $\gamma\lambda\ell^2 - 4(d_1 + d_2)(a + \lambda) > 0$ since $\ell_1 = \sqrt{\frac{d_1+d_2}{\frac{\gamma\lambda}{a+\lambda}}}$, $\ell_2 = 2\sqrt{\frac{d_1+d_2}{\frac{\gamma\lambda}{a+\lambda}}}$ and $\ell_1 < \ell_2 < \ell$. Furthermore, $K_0 < K_1 < K_2$.

Following the previous argument, for $\ell_n < \ell \leq \ell_{n+1}$, we have exactly $n + 1$ possible Hopf bifurcation points $K = K_j$ $j = 1, 2, \dots, n$ defined by $K_j = \frac{\gamma\lambda\ell^2(a+2\lambda)}{\gamma\lambda\ell^2 - j^2(d_1+d_2)(a+\lambda)}$, and these points satisfy that $K_0 < K_1 < K_2 < \dots < K_n$.

The next proposition shows that $D_n(K_j) > 0$ for all $n \in \mathbb{N} \cup \{0\}$, provided $\frac{M_*^2}{4d\gamma} \left(\frac{a+\lambda}{a}\right)^2 < \frac{d_1}{d_2}$.

Proposition 12. If $\frac{M_*^2}{4d\gamma} \left(\frac{a+\lambda}{a}\right)^2 < \frac{d_1}{d_2}$ then $D_n(K_j) > 0$ for all $n \in \mathbb{N} \cup \{0\}$, $j = 1, 2, \dots, n$.

Proof. It is easy to see that $M_* > \frac{\gamma\lambda(K-a-2\lambda)}{K(a+\lambda)}$ and $-M_* < -\frac{\gamma\lambda(K-a-2\lambda)}{K(a+\lambda)}$. Therefore, from (3.15) and (3.17), we have

$$D_n(K) > -d_2 M_* \left(\frac{n}{\ell}\right)^2 + d_1 d_2 \left(\frac{n}{\ell}\right)^4 + d\gamma \left(\frac{K-\lambda}{K}\right) \frac{a}{a+\lambda}.$$

On the other hand, since we are looking for bifurcation point K on the interval $[a + 2\lambda, \infty)$, we have $K > a + \lambda$. Hence, $-\frac{\lambda}{K} > -\frac{\lambda}{a+\lambda}$ and $\frac{K-\lambda}{K} > \frac{a}{a+\lambda}$, which implies that

$$D_n(K) > -d_2 M_* \left(\frac{n}{\ell}\right)^2 + d_1 d_2 \left(\frac{n}{\ell}\right)^4 + d\gamma \left(\frac{a}{a+\lambda}\right)^2.$$

Defining $\Psi(y) := -d_2 M_* y^2 + d_1 d_2 y^4 + d\gamma \left(\frac{a}{a+\lambda}\right)^2$, with $y = \frac{n}{\ell}$, we conclude that

$$\Psi(y) > 0 \text{ if } \frac{M_*^2}{4d\gamma} \left(\frac{a+\lambda}{a}\right)^2 < \frac{d_1}{d_2}.$$

□

Proposition 13. For the bifurcation values $K = K_j$ with $j = 1, 2, \dots, n$, we have

$$\begin{cases} \alpha_n(K_j) = 0 & \text{if } n = j, \\ \alpha_n(K_j) > 0 & \text{if } n < j, \\ \alpha_n(K_j) < 0 & \text{if } n > j. \end{cases}$$

We collect the above results and apply Theorem 1 to obtain the following Theorem:

Theorem 2. Assume that d_1, d_2, m and d are positive constants satisfying

$$\frac{M_*^2}{4d\gamma} \left(\frac{a+\lambda}{a} \right)^2 < \frac{d_1}{d_2}, \quad (3.19)$$

and ℓ_n as defined in (3.17). Then, for any $\ell \in (\ell_n, \ell_{n+1}]$, there exist $n+1$ points $K_j(\ell)$, $j = 0, 1, 2, \dots, n$, satisfying

$$K_0 < K_1 < K_2 < \dots < K_n,$$

such that systems (3.11)–(3.12) undergoes a Hopf bifurcation at these points.

i) The bifurcating periodic solutions from $K = K_0$ are spatially homogeneous, which coincides with the periodic solution of the corresponding ODE system.

ii) The bifurcating periodic solutions from $K = K_j$, $j = 1, 2, \dots, n$, are spatially non-homogeneous.

Next, we consider the bifurcation direction and stability of the bifurcating spatially homogeneous periodic solutions.

Theorem 3. Consider the one-parameter family of differential equations (3.11)–(3.12). The first Lyapunov coefficient associated with equilibrium E_0 for parameter values satisfying $K = K_0 = a + 2\lambda$ is given by $l_1(K_0) = -\frac{1}{\omega(K_0)} \frac{(\lambda+a)\gamma}{(a+\lambda)^2(a+2\lambda)}$. As $l_1(K_0) < 0$, the one-parameter family of differential equations (3.11)–(3.12) undergoes a supercritical codimension 1 Hopf bifurcation at $K = K_0$ and the bifurcating spatially homogeneous periodic solutions are locally asymptotically stable, which coincides with the periodic solution of the corresponding ODE system.

Proof. According to Theorem 1, to determine the stability and bifurcation direction of the bifurcating periodic solution, we shall calculate $\text{Re}(c_1(k_0))$, where $c_1(k_0)$ is given by (2.17). Note that

$$L_0(K_0) = \begin{pmatrix} 0 & -d \\ \frac{\gamma a}{(a+2\lambda)} & 0 \end{pmatrix} \text{ and } L_0^*(K_0) = \begin{pmatrix} 0 & \frac{\gamma a}{(a+2\lambda)} \\ -d & 0 \end{pmatrix}.$$

The eigenvalues associated with $L_0(K_0)$ are $\pm i\omega(K_0)$ where $\omega(K_0) = \omega_0 = \sqrt{\frac{d\gamma a}{(a+2\lambda)}}$; the eigenvectors of $L_0(K_0)$ and $L_0^*(K_0)$ are given by

$$q = \begin{pmatrix} 1 \\ -\frac{\omega_0}{d}i \end{pmatrix} = \begin{pmatrix} a_0 \\ c_0 \end{pmatrix} \text{ and } q^* = \frac{1}{2l\pi} \begin{pmatrix} 1 \\ \frac{-d}{\omega_0}i \end{pmatrix} = \begin{pmatrix} a_0^* \\ c_0^* \end{pmatrix},$$

respectively. Furthermore,

$$f_{uu}(0, 0, K_0) = \frac{-2\gamma\lambda}{(a+\lambda)(a+2\lambda)}, \quad f_{uv}(0, 0, K_0) = -\frac{ad}{\lambda(a+\lambda)}, \quad f_{vv}(0, 0, K_0) = 0, \quad g_{uu}(0, 0, K_0) = \frac{-2a\gamma}{(a+\lambda)(a+2\lambda)},$$

$$g_{uv}(0, 0, K_0) = \frac{da}{\lambda(a+\lambda)},$$

$$g_{vv}(0, 0, K_0) = 0, \quad f_{uuu}(0, 0, K_0) = -\frac{6a\gamma}{(a+\lambda)^2(a+2\lambda)}, \quad f_{uuv}(0, 0, K_0) = \frac{2ad}{\lambda(a+\lambda)^2},$$

$$g_{uuu}(0, 0, K_0) = \frac{6a\gamma}{(a+\lambda)^2(a+2\lambda)},$$

$$g_{uuv}(0, 0, K_0) = \frac{-2ad}{\lambda(a+\lambda)^2}, \quad g_{vvv}(0, 0, K_0) = g_{uvv}(0, 0, K_0) = 0, \quad f_{vvv}(0, 0, K_0) = f_{uvv}(0, 0, K_0) = 0.$$

Thus, we conclude that

$$B_{qq} = \begin{pmatrix} \delta_{10} \\ \zeta_{10} \end{pmatrix}; \quad B_{q\bar{q}} = \begin{pmatrix} \rho_{10} \\ \vartheta_{10} \end{pmatrix}; \quad C_{qq\bar{q}} = \begin{pmatrix} \sigma_{20} \\ \varrho_{20} \end{pmatrix},$$

where

$$\begin{aligned} \delta_{10} &= \frac{-2\gamma\lambda^2 + 2a\omega_0(a+2\lambda)i}{\lambda(a+\lambda)(a+2\lambda)}, & \zeta_{10} &= \frac{-2a\lambda\gamma - 2a(a+2\lambda)\omega_0 i}{\lambda(a+\lambda)(a+2\lambda)}, & \rho_{10} &= \frac{-2\gamma\lambda}{(a+\lambda)(a+2\lambda)}, \\ \vartheta_{10} &= \frac{-2a\gamma}{(a+\lambda)(a+2\lambda)}, & \sigma_{20} &= -\frac{6a\gamma}{(a+\lambda)^2(a+2\lambda)} - \frac{2a\omega_0 i}{\lambda(a+\lambda)^2}, & \varrho_{20} &= \frac{6a\gamma}{(a+\lambda)^2(a+2\lambda)} + \frac{2a\omega_0 i}{\lambda(a+\lambda)^2}. \end{aligned}$$

A straightforward calculation gives

$$\begin{aligned} \langle q^*, B_{qq} \rangle &= \left(\frac{ad}{\lambda(a+\lambda)} - \frac{\lambda\gamma}{(a+\lambda)(a+2\lambda)} \right) + \left(\frac{a\omega_0}{\lambda(a+\lambda)} + \frac{-a\gamma d}{\omega_0(a+\lambda)(a+2\lambda)} \right) i, & \langle q^*, B_{q\bar{q}} \rangle &= \left(\frac{-\gamma\lambda}{(a+\lambda)(a+2\lambda)} \right) + \left(\frac{a\gamma}{\omega_0(a+\lambda)(a+2\lambda)} \right) i, \\ \langle \bar{q}^*, B_{qq} \rangle &= \left(-\frac{ad}{\lambda(a+\lambda)} - \frac{\lambda\gamma}{(a+\lambda)(a+2\lambda)} \right) + \left(\frac{a\omega_0}{\lambda(a+\lambda)} + \frac{a\gamma d}{\omega_0(a+\lambda)(a+2\lambda)} \right) i, \\ \langle q^*, C_{qq\bar{q}} \rangle &= \left(-\frac{3a\gamma}{(a+\lambda)^2(a+2\lambda)} - \frac{ad}{\lambda(a+\lambda)^2} \right) + \left(\frac{3a\gamma d}{(a+\lambda)^2(a+2\lambda)\omega_0} - \frac{a\omega_0}{\lambda(a+\lambda)^2} \right) i. \end{aligned}$$

Thus, we calculate H_{20} and H_{11} as follows:

$$\begin{aligned} H_{20} &= \begin{pmatrix} \delta_{10} \\ \zeta_{10} \end{pmatrix} - \langle q^*, B_{qq} \rangle \begin{pmatrix} a_0 \\ c_0 \end{pmatrix} - \langle \bar{q}^*, B_{q\bar{q}} \rangle \begin{pmatrix} \bar{a}_0 \\ \bar{c}_0 \end{pmatrix} = 0, \\ H_{11} &= \begin{pmatrix} \rho_{10} \\ \vartheta_{10} \end{pmatrix} - \langle q^*, B_{q\bar{q}} \rangle \begin{pmatrix} a_0 \\ c_0 \end{pmatrix} - \langle \bar{q}^*, B_{qq} \rangle \begin{pmatrix} \bar{a}_0 \\ \bar{c}_0 \end{pmatrix} = 0. \end{aligned}$$

The previous equations imply that $r_{20} = r_{11} = 0$ and $\langle q^*, B_{r_{11}q} \rangle = \langle q^*, B_{r_{20}q} \rangle = 0$. Therefore,

$$\operatorname{Re} c_1(k_0) = \operatorname{Re} \left\{ \frac{i}{2\omega_0} \langle q^*, B_{qq} \rangle \langle q^*, B_{q\bar{q}} \rangle + \frac{1}{2} \langle q^*, C_{qq\bar{q}} \rangle \right\} = -\frac{(\lambda+a)\gamma}{(a+\lambda)^2(a+2\lambda)} < 0.$$

Now, since $\omega_0 > 0$ we conclude that $\frac{\operatorname{Re}\{c_1(K_0)\}}{\omega_0} < 0$. Hence, according to Theorem 1, the Hopf bifurcation is supercritical, and the bifurcating periodic solutions are locally asymptotically stable. \square

The bifurcation direction and stability of the spatially non-homogeneous bifurcating periodic solutions are determined in the following theorem.

Theorem 4. *The Hopf bifurcation for systems (3.11)–(3.12) at $K = K_j$, $j = 1, 2, \dots, n$, is supercritical if $\operatorname{Re}(c_1(K_j)) < 0$ and subcritical if $\operatorname{Re}(c_1(K_j)) > 0$, where $c_1(K_j)$ is given by (2.17). Furthermore, the bifurcating spatially non-homogeneous periodic solutions are stable (resp. unstable) if $\operatorname{Re}(c_1(K_j)) < 0$ (resp. if $\operatorname{Re}(c_1(K_j)) > 0$).*

Proof. Observe that

$$L(K) = \begin{pmatrix} d_1 \frac{\partial^2}{\partial x^2} + A(K) & B(K) \\ C(K) & d_2 \frac{\partial^2}{\partial x^2} + D(K) \end{pmatrix} \quad \text{and} \quad L_n(K) = \begin{pmatrix} A(K) - \frac{d_1 n^2}{\ell^2} & B(K) \\ C(K) & D(K) - \frac{d_2 n^2}{\ell^2} \end{pmatrix}$$

with

$$\begin{aligned} A(K) &= f_u(0, 0, K) = \frac{\lambda\gamma(K-a-2\lambda)}{K(a+\lambda)}, & B(K) &= f_v(0, 0, K) = -d, & C(K) &= g_u(0, 0, K) = \frac{\gamma(K-\lambda)a}{K(a+\lambda)} \\ \text{and } D(K) &= g_v(0, 0, K) = 0. \end{aligned}$$

For $n = j$ and $K = K_j$, we have

$$L_j(K_j) = \begin{pmatrix} \frac{d_2 j^2}{\ell^2} & -d \\ C(K_j) & -\frac{d_2 j^2}{\ell^2} \end{pmatrix} \quad \text{and} \quad L_j^*(K_j) = \begin{pmatrix} \frac{d_2 j^2}{\ell^2} & C(K_j) \\ -d & -\frac{d_2 j^2}{\ell^2} \end{pmatrix}$$

with eigenvalues given by $\pm i\omega_0 = \pm i \sqrt{dC(K_j) - \frac{d_2^2 j^4}{\ell^4}}$; and the respective eigenfunctions are given by

$$q = \cos\left(\frac{jx}{\ell}\right) \begin{pmatrix} a_j \\ c_j \end{pmatrix} = \cos\left(\frac{jx}{\ell}\right) \begin{pmatrix} 1 \\ \frac{d_2 j^2}{d\ell^2} - i\frac{\omega_0}{d} \end{pmatrix}, \quad \text{and} \quad q^* = \cos\left(\frac{jx}{\ell}\right) \begin{pmatrix} a_j^* \\ c_j^* \end{pmatrix} = \cos\left(\frac{jx}{\ell}\right) \begin{pmatrix} \frac{1}{\ell\pi} + \frac{d_2 j^2}{\omega_0 \pi \ell^3} i \\ -\frac{di}{\ell\pi\omega_0} \end{pmatrix},$$

which are obtained solving both equations $(L_j(K_j) - i\omega_0 I)q = 0$ and $(L_j^*(K_j) + i\omega_0 I)q^* = 0$. On the other hand, $n \neq 0$ implies that $\langle q^*, B_{qq} \rangle = \langle q^*, B_{q\bar{q}} \rangle = 0$, therefore

$$c_1(K_j) = \langle q^*, B_{r_{11}q} \rangle + \frac{1}{2} \langle q^*, B_{r_{20}\bar{q}} \rangle + \frac{1}{2} \langle q^*, C_{qq\bar{q}} \rangle.$$

Thus, the first Lyapunov coefficient is determined by calculating the quantities $\langle q^*, B_{r_{11}q} \rangle$; $\frac{1}{2} \langle q^*, B_{r_{20}\bar{q}} \rangle$; $\frac{1}{2} \langle q^*, C_{qq\bar{q}} \rangle$.

To obtain r_{20} and r_{11} , we solve the following equations:

$$\left[2i\omega_0 I - L_{2j}(K_j)\right]^{-1} = \frac{1}{\alpha_1 + \alpha_2 i} \begin{pmatrix} 2i\omega_0 + \frac{4d_2 j^2}{\ell^2} & -d \\ C(K_j) & 2i\omega_0 - \frac{(d_2 - 3d_1)j^2}{\ell^2} \end{pmatrix} \quad \text{where} \quad \alpha_1 = \frac{(12d_1 d_2 - 3d_2^2)j^4 - 3\ell^4 \omega_0^2}{\ell^4}$$

$$\text{and } \alpha_2 = 6\omega_0 \left(\frac{d_1 j^2 + d_2 j^2}{\ell^2}\right);$$

$$\left[2i\omega_0 I - L_0(K_j)\right]^{-1} = \frac{1}{\alpha_3 + i\alpha_4} \begin{pmatrix} 2i\omega_0 & -d \\ C(K_j) & 2i\omega_0 - \frac{(d_1 + d_2)j^2}{\ell^2} \end{pmatrix} \quad \text{where} \quad \alpha_3 = \frac{d_2^2 j^4 - 3\omega_0^2 \ell^4}{\ell^4}$$

$$\text{and } \alpha_4 = -\frac{2\omega_0(d_1 + d_2)j^2}{\ell^2};$$

$$\left[L_{2j}(K_j)\right]^{-1} = \frac{1}{\alpha_5} \begin{pmatrix} -\frac{4d_2 j^2}{\ell^2} & d \\ -C(K_j) & \frac{(d_2 - 3d_1)j^2}{\ell^2} \end{pmatrix} \quad \text{where} \quad \alpha_5 = \frac{\ell^4 \omega_0^2 + (12d_1 d_2 - 3d_2^2)j^4}{\ell^4};$$

$$\text{and} \quad \left[L_0(K_j)\right]^{-1} = \frac{1}{\beta C(K_j)} \begin{pmatrix} 0 & d \\ -C(K_j) & \frac{(d_1 + d_2)j^2}{\ell^2} \end{pmatrix}.$$

Thus, we obtain that

$$r_{20} = \frac{(\alpha_1 + \alpha_2 i)^{-1} \cos \frac{2jx}{\ell}}{2} \begin{pmatrix} \left(2i\omega_0 + \frac{4d_2 j^2}{\ell^2}\right) \delta_j - d\zeta_j \\ C(K_j)\delta_j + \left(2i\omega_0 - \frac{(d_2 - 3d_1)j^2}{\ell^2}\right) \zeta_j \end{pmatrix} + \frac{(\alpha_3 + i\alpha_4)^{-1}}{2} \begin{pmatrix} 2i\omega_0 \delta_j - d\zeta_j \\ C(K_j)\delta_j + \left(2i\omega_0 - \frac{(d_1 + d_2)j^2}{\ell^2}\right) \zeta_j \end{pmatrix} \quad (3.20)$$

and

$$r_{11} = \frac{\alpha_5^{-1} \cos \frac{2jx}{\ell}}{2} \begin{pmatrix} \frac{4d_2 j^2}{\ell^2} \rho_j - d\vartheta_j \\ C(K_j)\rho_j - \frac{(d_2 - 3d_1)j^2}{\ell^2} \vartheta_j \end{pmatrix} - \frac{1}{2dC(K_j)} \begin{pmatrix} d\vartheta_j \\ -C(K_j)\rho_j + \frac{(d_1 + d_2)j^2}{\ell^2} \vartheta_j \end{pmatrix}. \quad (3.21)$$

From (3.20) and (3.21), we conclude that r_{20} and r_{11} are given by

$$r_{20} = \begin{pmatrix} \xi \\ \eta \end{pmatrix} \cos \frac{2j}{\ell} x + \begin{pmatrix} \tau \\ \chi \end{pmatrix} \quad \text{and} \quad r_{11} = \begin{pmatrix} -\tilde{\xi} \\ -\tilde{\eta} \end{pmatrix} \cos \frac{2j}{\ell} x + \begin{pmatrix} \tilde{\tau} \\ \tilde{\chi} \end{pmatrix},$$

where

$$\begin{aligned} \xi &= \frac{(\alpha_1 + \alpha_2 i)^{-1}}{2} \left[\left(2i\omega_0 + \frac{4d_2 j^2}{\ell^2} \right) \delta_j - d\zeta_j \right]; \quad \eta = \frac{(\alpha_1 + \alpha_2 i)^{-1}}{2} \left[C(K_j) \delta_j + \left(2i\omega_0 - \frac{(d_2 - 3d_1)j^2}{\ell^2} \right) \zeta_j \right]; \\ \tau &= \frac{(\alpha_3 + i\alpha_4)^{-1}}{2} \left[2i\omega_0 \delta_j - d\zeta_j \right]; \quad \chi = \frac{(\alpha_3 + i\alpha_4)^{-1}}{2} \left[C(K_j) \delta_j + \left(2i\omega_0 - \frac{(d_1 + d_2)j^2}{\ell^2} \right) \zeta_j \right]; \\ \tilde{\xi} &= \frac{\alpha_5^{-1}}{2} \left(-\frac{4d_2 j^2}{\ell^2} \rho_j + d\vartheta_j \right); \quad \tilde{\eta} = \frac{\alpha_5^{-1}}{2} \left(-C(K_j) \rho_j + \frac{(d_2 - 3d_1)j^2}{\ell^2} \vartheta_j \right); \quad \tilde{\tau} = -\frac{\vartheta_j}{C(K_j)}; \quad \tilde{\chi} = -\frac{C(K_j) \rho_j + \frac{(d_1 + d_2)j^2}{\ell^2} \vartheta_j}{dC(K_j)}. \end{aligned}$$

On the other hand, note that at $(0, 0, K_j)$, we have

$$\begin{aligned} f_{uu} &= \frac{-2\gamma a^2 - 6\gamma a\lambda - 2\gamma\lambda^2 + 2\gamma K_j}{K_j(a+\lambda)^2} \quad ; \quad f_{uv} = -\frac{ad}{\lambda(a+\lambda)} \quad ; \quad f_{vv} = f_{vvv} = f_{uvv} = 0; \\ f_{uuu} &= -\frac{6a\gamma(K_j - \lambda)}{(a+\lambda)^3 K_j} \quad ; \quad f_{uuv} = \frac{2ad}{\lambda(a+\lambda)^2} \quad ; \quad g_{uu} = \frac{-2a\gamma(K_j - \lambda)}{(a+\lambda)^2 K_j}; \\ g_{uv} &= \frac{ad}{\lambda(a+\lambda)} \quad ; \quad g_{uuu} = \frac{6a\gamma(K_j - \lambda)}{K_j(a+\lambda)^3} \quad ; \quad g_{uuv} = \frac{-2a\gamma(K_j - \lambda)}{K_j(a+\lambda)^2}; \\ g_{vv} &= g_{uvv} = 0 \quad ; \quad g_{vvv} = 0. \end{aligned}$$

As we know that

$$\bar{q} = \begin{pmatrix} \bar{a}_j \\ \bar{c}_j \end{pmatrix} \cos\left(\frac{jx}{\ell}\right) = \begin{pmatrix} 1 \\ \frac{d_2 j^2}{d\ell^2} + i\frac{\omega_0}{d} \end{pmatrix} \cos\left(\frac{jx}{\ell}\right),$$

we obtain

$$B(r_{20}, \bar{q}) = \begin{pmatrix} f_{uu}\xi + f_{uv}\eta + f_{uv}\xi\bar{c}_j \\ g_{uu}\xi + g_{uv}\eta + g_{uv}\xi\bar{c}_j \end{pmatrix} \cos\left(\frac{2jx}{\ell}\right) \cos\left(\frac{jx}{\ell}\right) + \begin{pmatrix} f_{uu}\tau + f_{uv}\chi + f_{uv}\bar{c}_j\tau \\ g_{uu}\tau + g_{uv}\chi + g_{uv}\bar{c}_j\tau \end{pmatrix} \cos\left(\frac{jx}{\ell}\right),$$

and

$$B(r_{11}, q) = \begin{pmatrix} f_{uu}\tilde{\xi} + f_{uv}\tilde{\eta} + f_{uv}c_j\tilde{\xi} \\ g_{uu}\tilde{\xi} + g_{uv}\tilde{\eta} + g_{uv}c_j\tilde{\xi} \end{pmatrix} \cos\left(\frac{2jx}{\ell}\right) \cos\left(\frac{jx}{\ell}\right) + \begin{pmatrix} f_{uu}\tilde{\tau} + f_{uv}\tilde{\chi} + f_{uv}c_j\tilde{\tau} \\ g_{uu}\tilde{\tau} + g_{uv}\tilde{\chi} + g_{uv}c_j\tilde{\tau} \end{pmatrix} \cos\left(\frac{jx}{\ell}\right).$$

Now, from (2.12), it follows that:

$$\begin{aligned} \delta_{1j} &= f_{uu} - 2\frac{i\omega_0}{d} f_{uv} \quad ; \quad \rho_{1j} = f_{uu} \quad ; \quad \sigma_{2j} = f_{uuu} - \frac{i\omega_0}{d} f_{uuv}; \\ \zeta_{1j} &= g_{uu} - 2\frac{i\omega_0}{d} g_{uv} \quad ; \quad \varrho_{1j} = g_{uu} \quad ; \quad \vartheta_{2j} = g_{uuu} - \frac{i\omega_0}{d} g_{uuv}. \end{aligned}$$

Since for all $n \neq 0$

$$\int_0^{\ell\pi} \cos^2\left(\frac{nx}{\ell}\right) dx = \frac{\ell\pi}{2} \quad , \quad \int_0^{\ell\pi} \cos\left(\frac{2nx}{\ell}\right) \cos^2\left(\frac{nx}{\ell}\right) dx = \frac{\ell\pi}{4} \quad , \quad \int_0^{\ell\pi} \cos^4\left(\frac{nx}{\ell}\right) dx = \frac{3\ell\pi}{8},$$

the expressions for $\langle q^*, B_{r_{20\bar{q}}} \rangle$, $\langle q^*, B_{r_{11q}} \rangle$, and $\langle q^*, C_{qq\bar{q}} \rangle$ are given by

$$\begin{aligned} \langle q^*, B_{r_{20\bar{q}}} \rangle &= \frac{\ell\pi}{4} \bar{a}_j^* (f_{uu}\xi + f_{uv}\eta + f_{uv}\xi\bar{c}_j) + \frac{\ell\pi}{4} \bar{c}_j^* (g_{uu}\xi + g_{uv}\eta + g_{uv}\xi\bar{c}_j) + \frac{\ell\pi}{2} \bar{a}_j^* (f_{uu}\tau + f_{uv}\chi + f_{uv}\bar{c}_j\tau) \\ &\quad + \frac{\ell\pi}{2} \bar{c}_j^* (g_{uu}\tau + g_{uv}\chi + g_{uv}\bar{c}_j\tau), \end{aligned} \quad (3.22)$$

$$\begin{aligned} \langle q^*, B_{r_{11q}} \rangle &= \frac{\ell\pi}{4} \bar{a}_j^* (f_{uu}\xi + f_{uv}\eta + f_{uv}\xi\bar{c}_j) + \frac{\ell\pi}{4} \bar{c}_j^* (g_{uu}\xi + g_{uv}\eta + g_{uv}\xi\bar{c}_j) + \frac{\ell\pi}{2} \bar{a}_j^* (f_{uu}\tau + f_{uv}\chi + f_{uv}\bar{c}_j\tau) \\ &\quad + \frac{\ell\pi}{2} \bar{c}_j^* (g_{uu}\tilde{\tau} + g_{uv}\tilde{\chi} + g_{uv}c_j\tilde{\tau}), \end{aligned} \quad (3.23)$$

and

$$\langle q^*, C_{qq\bar{q}} \rangle = \frac{3\ell\pi}{8} (\bar{a}_j^* \sigma_j + \bar{c}_j^* \varrho_j). \quad (3.24)$$

The expressions for ξ , η , τ , and χ can be written in the form $\xi = \xi_R + i\xi_I$, $\eta = \eta_R + i\eta_I$, $\tau = \tau_R + i\tau_I$, and $\chi = \chi_R + i\chi_I$, respectively, where

$$\begin{aligned} \xi_R &= \frac{\alpha_1}{2(\alpha_1^2 + \alpha_2^2)} \left(\frac{4d_2 j^2}{\ell^2} f_{uu} + \frac{4\omega_0^2}{d} f_{uv} - dg_{uu} \right) + \frac{\alpha_2}{2(\alpha_1^2 + \alpha_2^2)} \left(2\omega_0 f_{uu} - \frac{8\omega_0 d_2 j^2}{d\ell^2} f_{uv} + 2\omega_0 g_{uv} \right), \\ \xi_I &= \frac{\alpha_1}{2(\alpha_1^2 + \alpha_2^2)} \left(2\omega_0 f_{uu} - \frac{8\omega_0 d_2 j^2}{d\ell^2} f_{uv} + 2\omega_0 g_{uv} \right) - \frac{\alpha_2}{2(\alpha_1^2 + \alpha_2^2)} \left(\frac{4d_2 j^2}{\ell^2} f_{uu} + 4\frac{\omega_0^2}{d} f_{uv} - dg_{uu} \right), \\ \eta_R &= \frac{\alpha_1}{2(\alpha_1^2 + \alpha_2^2)} \left(C(K_j) f_{uu} - \frac{(d_2 - 3d_1)j^2}{\ell^2} g_{uu} + 4\frac{\omega_0^2}{d} g_{uv} \right) + \frac{\alpha_2}{2(\alpha_1^2 + \alpha_2^2)} \left(2\omega_0 g_{uu} - 2C(K_j) \frac{\omega_0}{d} f_{uv} + 2\frac{(d_2 - 3d_1)\omega_0 j^2}{\ell^2 d} g_{uv} \right), \\ \eta_I &= \frac{\alpha_1}{2(\alpha_1^2 + \alpha_2^2)} \left(2\omega_0 g_{uu} - 2C(K_j) \frac{\omega_0}{d} f_{uv} + 2\frac{(d_2 - 3d_1)\omega_0 j^2}{\ell^2 d} g_{uv} \right) - \frac{\alpha_2}{2(\alpha_1^2 + \alpha_2^2)} \left(C(K_j) f_{uu} - \frac{(d_2 - 3d_1)j^2}{\ell^2} g_{uu} + 4\frac{\omega_0^2}{d} g_{uv} \right), \\ \tau_R &= \frac{\alpha_3}{2(\alpha_3^2 + \alpha_4^2)} \left(4\frac{\omega_0^2}{d} f_{uv} - dg_{uu} \right) + \frac{\alpha_4}{2(\alpha_3^2 + \alpha_4^2)} (2\omega_0 f_{uu} + 2\omega_0 g_{uv}), \\ \tau_I &= \frac{\alpha_3}{2(\alpha_3^2 + \alpha_4^2)} (2\omega_0 f_{uu} + 2\omega_0 g_{uv}) - \frac{\alpha_4}{2(\alpha_3^2 + \alpha_4^2)} \left(4\frac{\omega_0^2}{d} f_{uv} - dg_{uu} \right), \\ \chi_R &= \frac{\alpha_3}{2(\alpha_3^2 + \alpha_4^2)} \left(C(K_j) f_{uu} - \frac{(d_1 + d_2)j^2}{\ell^2} g_{uu} + 4\omega_0^2 \frac{g_{uv}}{d} \right) + \frac{\alpha_4}{2(\alpha_3^2 + \alpha_4^2)} \left(2\omega_0 g_{uu} + 2\frac{(d_1 + d_2)j^2 \omega_0}{\ell^2 d} g_{uv} - 2C(K_j) \frac{\omega_0}{d} f_{uv} \right), \\ \chi_I &= \frac{\alpha_3}{2(\alpha_3^2 + \alpha_4^2)} \left(2\omega_0 g_{uu} + 2\frac{(d_1 + d_2)j^2 \omega_0}{\ell^2 d} g_{uv} - 2C(K_j) \frac{\omega_0}{d} f_{uv} \right) - \frac{\alpha_4}{2(\alpha_3^2 + \alpha_4^2)} \left(C(K_j) f_{uu} - \frac{(d_1 + d_2)j^2}{\ell^2} g_{uu} + 4\omega_0^2 \frac{g_{uv}}{d} \right). \end{aligned}$$

Furthermore, the expressions for $\tilde{\xi}$, $\tilde{\eta}$, $\tilde{\tau}$, and $\tilde{\chi}$ are given by

$$\begin{aligned} \tilde{\xi} &= \frac{\alpha_5^{-1}}{2} \left(-\frac{4d_2 j^2}{\ell^2} \rho_j + d\vartheta_j \right), \\ \tilde{\eta} &= \frac{\alpha_5^{-1}}{2} \left(-C(K_j) \rho_j + \frac{(d_3 - 3d_1)j^2}{\ell^2} \vartheta_j \right), \\ \tilde{\tau} &= -\frac{\vartheta_j}{C(K_j)}, \\ \tilde{\chi} &= -\frac{C(K_1) \rho_j + \frac{(d_1 + d_2)j^2}{\ell^2} \vartheta_j}{dC(K_j)}. \end{aligned}$$

Thus, the real part of $\langle q^*, C_{qq\bar{q}} \rangle$, $\langle q^*, B_{r_{20}\bar{q}} \rangle$, and $\langle q^*, B_{r_{11}q} \rangle$ are given by

$$\begin{aligned} \operatorname{Re} \langle q^*, C_{qq\bar{q}} \rangle &= \frac{3}{8} \left[f_{uuu} - \frac{d_2 j^2}{d \ell^2} f_{uuv} + g_{uuv} \right], \\ \operatorname{Re} \langle q^*, B_{r_{20}\bar{q}} \rangle &= \frac{1}{4} \left[f_{uu} \xi_R + f_{uv} \eta_R + \frac{f_{uu} \xi_I d_2 j^2}{\omega_0 \ell^2} + \frac{f_{uv} \eta_I d_2 j^2}{\omega_0 \ell^2} - \frac{g_{uu} \xi_I d}{\omega_0} - \frac{g_{uv} \eta_I d}{\omega_0} \right] \\ &\quad + \frac{1}{4} \left[\frac{f_{uv} \xi_R d_2 j^2}{d \ell^2} - \frac{f_{uv} \xi_I \omega_0}{d} + \frac{f_{uv} \xi_R d_2 j^2}{d \ell^2} + \frac{f_{uv} \xi_I d_2^2 j^4}{d \omega_0 \ell^4} - g_{uv} \xi_R - \frac{g_{uv} \xi_I d_2 j^2}{\omega_0 \ell^2} \right] \\ &\quad + \frac{1}{4} \left(2f_{uu} \tau_R + 2f_{uv} \chi_R + \frac{2f_{uu} \tau_I d_2 j^2}{\omega_0 \ell^2} + \frac{2f_{uv} \tau_I d_2^2 j^4}{d \omega_0 \ell^4} \right) \\ &\quad + \frac{1}{4} \left(\frac{2f_{uv} \chi_I d_2 j^2}{\omega_0 \ell^2} + \frac{2f_{uv} \tau_R d_2 j^2}{d \ell^2} + \frac{2f_{uv} \tau_R d_2 j^2}{d \ell^2} - \frac{2f_{uv} \tau_I \omega_0}{d} \right) \\ &\quad - \frac{1}{4} \left(\frac{2g_{uu} \tau_I d}{\omega_0} + \frac{2g_{uv} \chi_I d}{\omega_0} + \frac{2g_{uv} \tau_I d_2 j^2}{\omega_0 \ell^2} + 2g_{uv} \tau_R \right), \\ \operatorname{Re} \langle q^*, B_{r_{11}q} \rangle &= \frac{1}{4} \left[f_{uu} \tilde{\xi} + f_{uv} \tilde{\eta} + g_{uv} \tilde{\xi} \right] + \frac{1}{4} \left[2f_{uu} \tilde{\tau} + 2f_{uv} \tilde{\chi} + 2g_{uv} \tilde{\tau} \right] \\ &= \frac{1}{4} \left[f_{uu} \tilde{\xi} + 2f_{uu} \tilde{\tau} + f_{uv} \tilde{\eta} + 2f_{uv} \tilde{\chi} + g_{uv} \tilde{\xi} + 2g_{uv} \tilde{\tau} \right] \\ &= \frac{1}{4} \left[f_{uu} (\tilde{\xi} + 2\tilde{\tau}) + f_{uv} (\tilde{\eta} + 2\tilde{\chi}) + g_{uv} (\tilde{\xi} + 2\tilde{\tau}) \right]. \end{aligned}$$

Therefore,

$$\begin{aligned} \operatorname{Re} [c_1(K_j)] &= \operatorname{Re} \langle q^*, B_{r_{11}q} \rangle + \frac{1}{2} \operatorname{Re} \langle q^*, B_{r_{20}\bar{q}} \rangle + \frac{1}{2} \operatorname{Re} \langle q^*, C_{qq\bar{q}} \rangle \\ &= \frac{1}{4} f_{uu} (\tilde{\xi} + 2\tilde{\tau}) + \frac{1}{4} f_{uv} (\tilde{\eta} + 2\tilde{\chi}) + \frac{1}{4} g_{uv} (\tilde{\xi} + 2\tilde{\tau}) + \frac{1}{4} \frac{d_2 j^2}{d \ell^2} f_{uv} (\xi_R + 2\tau_R) + \frac{1}{8} f_{uu} (\xi_R + 2\tau_R) \\ &\quad + \frac{1}{8} f_{uv} (\eta_R + 2\chi_R) - \frac{1}{8} g_{uv} (\xi_R + 2\tau_R) - \frac{1}{8} \frac{\omega_0}{d} f_{uv} (\xi_I + 2\tau_I) + \frac{1}{8} \frac{d_2 j^2}{\omega_0 \ell^2} f_{uu} (\xi_I + 2\tau_I) \\ &\quad + \frac{1}{8} \frac{d_2 j^2}{\omega_0 \ell^2} f_{uv} (\eta_I + 2\chi_I) - \frac{1}{8} \frac{d_2 j^2}{\omega_0 \ell^2} g_{uv} (\xi_I + 2\tau_I) + \frac{1}{8} \frac{d_2^2 j^4}{\omega_0 \ell^2} \frac{(f_{uv} \xi_I + 2f_{uv} \tau_I)}{d} \\ &\quad - \frac{d}{8\omega_0} [g_{uu} (\xi_I + 2\tau_I) + g_{uv} (\eta_I + 2\chi_I)] + \frac{3}{16} \left[f_{uuu} - \frac{d_2 j^2}{d \ell^2} f_{uuv} + g_{uuv} \right], \end{aligned} \quad (3.25)$$

As we show in Proposition 11, $\alpha'_n(K) > 0$ for $n = 0, 1, 2, \dots$ and $K \in [K_0, \infty)$. Hence, according to Theorem 1, the Hopf bifurcation is supercritical if $\operatorname{Re} (c_1(K_j)) < 0$ and subcritical if $\operatorname{Re} (c_1(K_j)) > 0$. Furthermore, the bifurcating spatially non-homogeneous periodic solutions are stable (resp. unstable) if $\operatorname{Re} (c_1(K_j)) < 0$ (resp. if $\operatorname{Re} (c_1(K_j)) > 0$). \square

The following example illustrates the analytical results obtained in this section regarding the codimension 1 Hopf bifurcation, when the bifurcating spatially non-homogeneous periodic solutions are stable. It is worth noting that obtaining $\operatorname{Re} (c_1(K_j)) < 0$ and $\operatorname{Re} (c_1(K_j)) > 0$, leads to the occurrence of a degenerated Hopf bifurcation when $\operatorname{Re} (c_1(K_j)) = 0$. We do not consider the case where the bifurcating spatially non-homogeneous periodic solutions are unstable since we could not fit the data to get $\operatorname{Re} (c_1(K_j)) > 0$. Thus, the system may not present a degenerated Hopf bifurcation.

Example 1. If we consider the following values of the parameters $d_1 = 0.5$, $d_2 = 0.5$, $m = 0.9$, $a = 0.6$, $\gamma = 0.9$, $d = 0.3$, and $\lambda = 0.3$, we get $K_0 = 1.2$, $\ell_n = 1.825n$, and therefore, condition (3.19) is satisfied, which implies $D_n(K_j) > 0$ for all $n \in \mathbb{N} \cup \{0\}$, $j = 1, 2, 3, \dots, n$.

- For $n = 1$, we choose $\ell = 2.5 \in (\ell_1, \ell_2] \approx (1.825; 3.651]$. Solving the equation $\frac{0.3(K-1.2)}{K} - \frac{1}{2.5^2} = 0$ we get $K_1 = 2.57$. Therefore, the Hopf bifurcation points are $\{K_0, K_1\} = \{1.2, 2.57\}$.

For $K_0 = 1.2$, we get $\omega(K_0) = 0.1837$ and $l_1(K_0) \simeq -2.26 < 0$.

For $K_1 = 2.57$, we obtain the following:

$$\begin{aligned} f_{uu} &= 0.4778 & f_{uv} &= -0.6667 & f_{uuu} &= -3.9259 & f_{uuv} &= 1.4815 \\ g_{uu} &= -1.1778 & g_{uv} &= 0.6667 & g_{uuu} &= 3.9259 & g_{uuv} &= -1.1778 \\ f_{vv} &= g_{vv} = 0 & f_{vvv} &= g_{vvv} = 0 & f_{vvv} &= g_{vvv} = 0; \end{aligned}$$

$$q = \cos\left(\frac{jx}{\ell}\right) \left(\frac{1}{\frac{d_2 j^2}{d\ell^2} - i\frac{\omega_0}{d}} \right) ; \quad q^* = \cos\left(\frac{jx}{\ell}\right) \left(\frac{1}{\ell\pi} + \frac{\frac{d_2 j^2}{\omega_0 \pi \ell^3} i}{-\frac{di}{\ell\pi\omega_0}} \right).$$

Furthermore, we have

$$\begin{aligned} (2i\omega_0 I - L_{2j}(K_j))^{-1} &= \frac{1}{\alpha_1 + \alpha_2 i} \begin{pmatrix} 2i\omega_0 + \frac{d_2 4j^2}{\ell^2} & -d \\ C(K_j) & 2i\omega_0 - (d_2 - 3d_1) \frac{j^2}{\ell^2} \end{pmatrix} \\ (2i\omega_0 I - L_0(K_j))^{-1} &= \frac{1}{\alpha_3 + \alpha_4 i} \begin{pmatrix} 2i\omega_0 + \frac{d_2 4j^2}{\ell^2} & -d \\ C(K_j) & 2i\omega_0 - (d_2 - 3d_1) \frac{j^2}{\ell^2} \end{pmatrix} \end{aligned}$$

where

$$\begin{aligned} \omega_0 &= 0.3906 ; \quad C(2.57) = 0.5300 ; \quad \alpha_1 = -0.4002; \\ \alpha_2 &= 0.3750 ; \quad \alpha_3 = -0.4514 ; \quad \alpha_4 = -0.1250; \\ \alpha_5 &= 0.2102 ; \quad \alpha_1^2 + \alpha_2^2 = 0.30079 ; \quad \alpha_3^2 + \alpha_4^2 = 0.21939; \end{aligned}$$

$$\begin{aligned} \delta_j &= 0.4778 + 1.7362i; \quad \rho_j = 0.4778; \quad \sigma_j = -3.9259 - 1.9291i; \\ \zeta_j &= -1.1778 - 1.7362i; \quad \varrho_j = -1.1778; \quad \vartheta_j = 3.9259 + 1.5336i; \end{aligned}$$

and

$$\begin{aligned} \xi_R &= 1.4693 ; \quad \xi_I = -0.4344 ; \quad \eta_R = -1.1186 ; \quad \eta_I = -0.7012; \\ \tau_R &= 0.7772 ; \quad \tau_I = -1.2056 ; \quad \chi_R = -1.9290 ; \quad \chi_I = 0.2265; \\ \tilde{\xi} &= -1.2041 ; \quad \tilde{\eta} = -0.1541; \quad \tilde{\tau} = 2.2222 ; \quad \tilde{\chi} = -0.4074. \end{aligned}$$

Consequently, determining the quantities $r_{20}, r_{11}, \langle q^*, B_{r_{11}q} \rangle, \langle q^*, B_{r_{11}q} \rangle$, and $\langle q^*, C_{qq\bar{q}} \rangle$, and plugging the obtained results in (3.25), we get

$$\begin{aligned} \operatorname{Re}[c_1(K_1)] &= \operatorname{Re}\langle q^*, B_{r_{11}q} \rangle + \frac{1}{2} \operatorname{Re}\langle q^*, B_{r_{20}\bar{q}} \rangle + \frac{1}{2} \operatorname{Re}\langle q^*, C_{qq\bar{q}} \rangle \\ &= -0.0140 < 0. \end{aligned}$$

Hence,

$$l_1(2.57) = -0.0358 < 0.$$

- For $n = 2$ and $j = 1, 2$ we have $\ell = 5.0 \in (\ell_2, \ell_3] \approx (3.651, 5.477]$. Solving the equation $\frac{0.3(K-1.2)}{K} - 0.04 = 0$ we get $K_1 = 1.3846$. likewise, solving the equation $\frac{0.3(K-1.2)}{K} - 0.16 = 0$ we get $K_2 = 2.5714$. therefore, the Hopf bifurcation points are $\{K_0, K_1, K_2\} = \{1.2, 1.3846, 2.5714\}$. For $K_0 = 1.2$, we obtain $\omega(K_0) = 0.1837$ and consequently, $l_1(1.2) \simeq -2.26 < 0$. For $K_1 = 1.3846$, we obtain the following:

$$\begin{aligned} f_{uu} &= -0.2556 ; \quad f_{uv} = -0.6667 ; \quad f_{uuu} = -3.4815 ; \quad f_{uuv} = 1.4815 \\ g_{uu} &= -1.0444 ; \quad g_{uv} = 0.6667 ; \quad g_{uuu} = 3.4815 ; \quad g_{uuv} = -1.0444 \\ f_{vv} &= g_{vv} = 0 ; \quad f_{uvv} = g_{uvv} = 0 ; \quad f_{vvv} = g_{vvv} = 0; \end{aligned}$$

$$q = \cos\left(\frac{jx}{\ell}\right) \begin{pmatrix} 1 \\ \frac{d_3 j^2}{\beta \ell^2} - i \frac{\omega_0}{\beta} \end{pmatrix} ; \quad q^* = \cos\left(\frac{jx}{\ell}\right) \begin{pmatrix} \frac{1}{\ell\pi} + \frac{d_3 j^2}{\omega_0 \pi \ell^3} i \\ -\frac{\beta_2 i}{\ell \pi \omega_0} \end{pmatrix}.$$

Furthermore, we have

$$\begin{aligned} (2i\omega_0 I - L_{2j}(K_j))^{-1} &= \frac{1}{\alpha_1 + \alpha_2 i} \begin{pmatrix} 2i\omega_0 + \frac{d_2 4j^2}{\ell^2} & -d \\ C(K_j) & 2i\omega_0 - (d_2 - 3d_1) \frac{j^2}{\ell^2} \end{pmatrix} \\ (2i\omega_0 I - L_0(K_j))^{-1} &= \frac{1}{\alpha_3 + \alpha_4 i} \begin{pmatrix} 2i\omega_0 + \frac{d_2 4j^2}{\ell^2} & -d \\ C(K_j) & 2i\omega_0 - (d_2 - 3d_1) \frac{j^2}{\ell^2} \end{pmatrix} \end{aligned}$$

where

$$\begin{aligned} \omega_0 &= 0.3750; & C(1.3846) &= 0.4700; & \alpha_1 &= -0.4182; \\ \alpha_2 &= 0.0900; & \alpha_1^2 + \alpha_2^2 &= 0.18299; & \alpha_3 &= -0.4214; \\ \alpha_4 &= -0.0300; & \alpha_3^2 + \alpha_4^2 &= 0.17848; & \alpha_5 &= -144.0008; \end{aligned}$$

$$\begin{aligned} \delta_j &= -0.2556 + 1.6665i; & \rho_j &= -0.2556; & \sigma_j &= -3.4815 - 1.8517i; \\ \zeta_j &= -1.0444 - 1.6665i; & \varrho_j &= -1.0444; & \vartheta_j &= 3.4815 + 1.3054i; \end{aligned}$$

and

$$\begin{aligned} \xi_R &= 1.2020 & \xi_I &= -0.2693 & \eta_R &= -1.2595 & \eta_I &= -0.1913; \\ \tau_R &= 1.0796 & \tau_I &= -0.4427 & \chi_R &= -1.3885 & \chi_I &= 0.0197; \\ \tilde{\xi} &= -1.0156 & \tilde{\eta} &= 0.5613 & \tilde{\tau} &= 2.2222 & \tilde{\chi} &= 1.1481. \end{aligned}$$

Consequently, determining the quantities $r_{20}, r_{11}, \langle q^*, B_{r_{11}q} \rangle, \langle q^*, B_{r_{11}\bar{q}} \rangle$, and $\langle q^*, C_{qq\bar{q}} \rangle$, and plugging the obtained results in (3.25), we get

$$\begin{aligned} \operatorname{Re}[c_1(K_1)] &= \operatorname{Re}\langle q^*, B_{r_{11}q} \rangle + \frac{1}{2} \operatorname{Re}\langle q^*, B_{r_{20}\bar{q}} \rangle + \frac{1}{2} \operatorname{Re}\langle q^*, C_{qq\bar{q}} \rangle \\ &= -2.4335. \end{aligned}$$

Hence,

$$l_1(1.3846) = -6.4893 < 0.$$

For $K_2 = 2.5714$, we have

$$\begin{aligned} f_{uu} &= 0.4778 & f_{uv} &= -0.6667 & f_{uuu} &= -3.9259 & f_{uuv} &= 1.4815 \\ g_{uu} &= -1.1778 & g_{uv} &= 0.6667 & g_{uuu} &= -1.1778 & g_{uuv} &= 3.9259 \\ f_{vv} &= g_{vv} = 0 & f_{uvv} &= g_{uvv} = 0 & f_{vvv} &= g_{vvv} = 0; \end{aligned}$$

$$q = \cos\left(\frac{jx}{\ell}\right) \begin{pmatrix} 1 \\ \frac{d_2 j^2}{d \ell^2} - i \frac{\omega_0}{d} \end{pmatrix} ; \quad q^* = \cos\left(\frac{jx}{\ell}\right) \begin{pmatrix} \frac{1}{\ell\pi} + \frac{d_2 j^2}{\omega_0 \pi \ell^3} i \\ -\frac{d i}{\ell \pi \omega_0} \end{pmatrix}.$$

Furthermore,

$$(2i\omega_0 I - L_{2j}(K_j))^{-1} = \frac{1}{\alpha_1 + \alpha_2 i} \begin{pmatrix} 2i\omega_0 + \frac{d_2 4j^2}{\ell^2} & -d \\ C(K_j) & 2i\omega_0 - (d_2 - 3d_1) \frac{j^2}{\ell^2} \end{pmatrix}$$

$$(2i\omega_0 I - L_0(K_j))^{-1} = \frac{1}{\alpha_3 + \alpha_4 i} \begin{pmatrix} 2i\omega_0 + \frac{d_2 4j^2}{\ell^2} & -d \\ C(K_j) & 2i\omega_0 - (d_2 - 3d_1) \frac{j^2}{\ell^2} \end{pmatrix}$$

where

$$\begin{aligned} \omega_0 &= 0.3906; & C(2.5714) &= 0.5300; & \alpha_1 &= -0.4002; \\ \alpha_2 &= 0.3750; & \alpha_1^2 + \alpha_2^2 &= 0.30079; & \alpha_3 &= -0.4514; \\ \alpha_4 &= -0.1250; & \alpha_3^2 + \alpha_4^2 &= 0.21939; & \alpha_5 &= 0.2102; \end{aligned}$$

$$\begin{aligned} \delta_j &= 0.4778 + 1.7362i; & \rho_j &= 0.4778; & \sigma_j &= -3.9259 - 1.9291i; \\ \zeta_j &= -1.1778 - 1.7362i; & \varrho_j &= -1.1778; & \vartheta_j &= 3.9259 + 1.5336ii; \end{aligned}$$

and

$$\begin{aligned} \xi_R &= 1.4693; & \xi_I &= -0.4344; & \eta_R &= -1.1186; & \eta_I &= -0.7012; \\ \tau_R &= 0.7772; & \tau_I &= -1.2056; & \chi_R &= -1.9290; & \chi_I &= 0.2265; \\ \tilde{\xi} &= -1.2041; & \tilde{\eta} &= -0.1541; & \tilde{\tau} &= 2.2222; & \tilde{\chi} &= -0.4074. \end{aligned}$$

Consequently, determining the quantities $r_{20}, r_{11}, \langle q^*, B_{r_{11}q} \rangle, \langle q^*, B_{r_{11}\bar{q}} \rangle$, and $\langle q^*, C_{qq\bar{q}} \rangle$, and plugging the obtained results in (3.25), we get

$$\begin{aligned} \operatorname{Re}[c_1(K_2)] &= \operatorname{Re} \langle q^*, B_{r_{11}q} \rangle + \frac{1}{2} \operatorname{Re} \langle q^*, B_{r_{20}\bar{q}} \rangle + \frac{1}{2} \operatorname{Re} \langle q^*, C_{qq\bar{q}} \rangle \\ &= -1.1445 < 0. \end{aligned}$$

Hence,

$$l_1(2.5714) = -2.9301 < 0.$$

Remark 5. As mentioned, the results concerning the Hopf bifurcation for the corresponding ODE version of systems (1.1)–(1.2), were obtained in [14] (see also [26]). We note that the results presented, can also be obtained for systems (1.1)–(1.2) restricted to the u, w plane, as obtained in [14] Theorem 3.3 pp. 1304, for the ODE version of systems (1.1)–(1.2). However, the calculations are analogous and we do not present them here.

4. Numerical simulations

We use several numerical simulations to illustrate and complement our analytical results. The simulations are generated by using the Matlab pdepe solver, which solves initial-boundary value problems for parabolic-elliptic PDEs in 1-D. We have identified a critical parameter values for the systems (3.11)–(3.12) namely, $K = K_0 = a + 2\lambda$. This is the smallest Hopf bifurcation point.

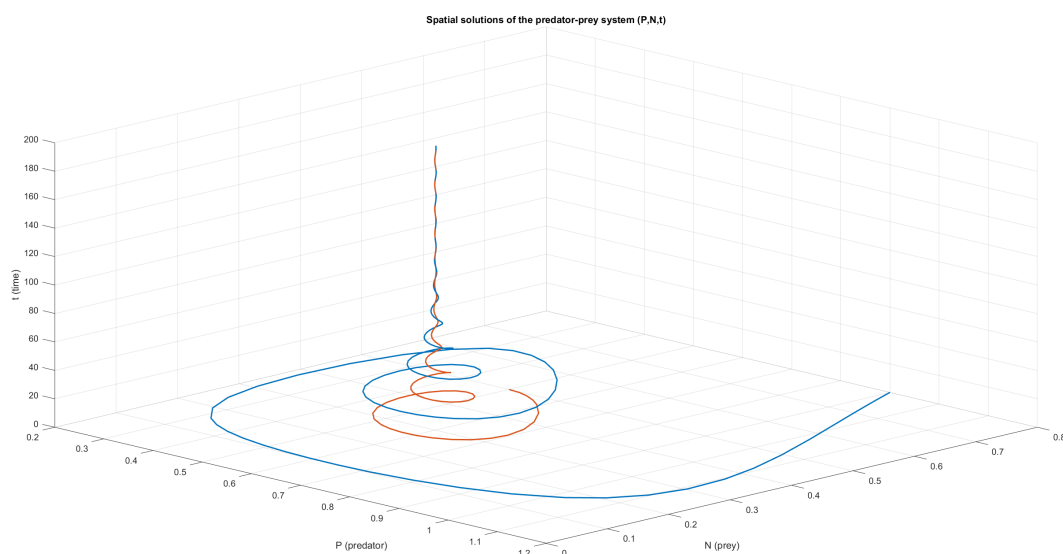


Figure 1. Numerical simulation for the ODE version of systems (1.1)–(1.2): $u(t)$; $v(t)$. We consider the following values of parameters: $n = 0, K = 0.9, a = 0.6, \gamma = 0.9, m = 0.9, d = 0.3$, and $\lambda = 0.3$, where the initial condition are taken at $(0.8, 0.9)$ and $(0.5, 0.5)$. The equilibrium solution $E = (0.3, 0.6)$ is asymptotically stable.

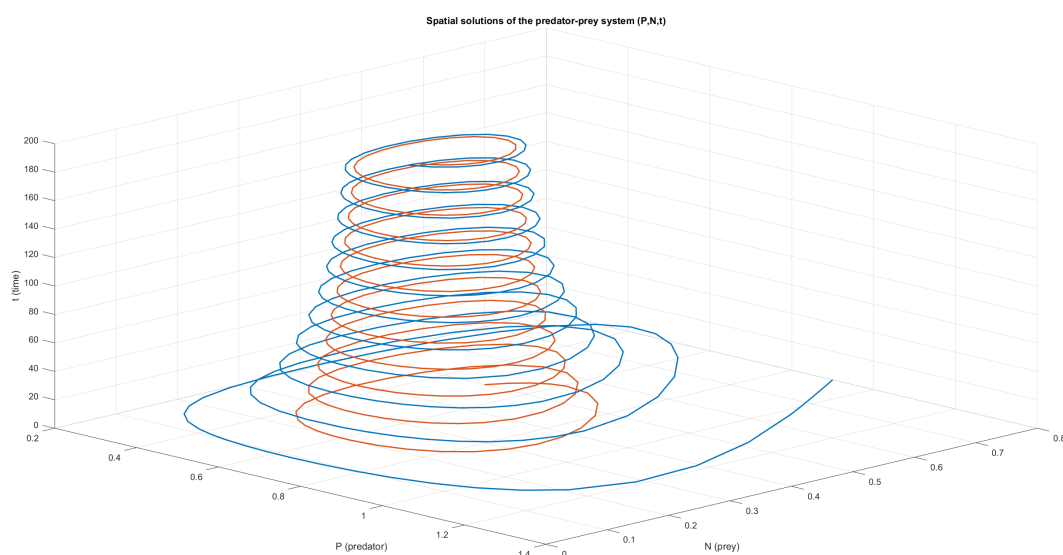


Figure 2. Numerical simulation for the ODE version of systems (1.1)–(1.2): $u(t)$; $v(t)$. We consider the following values of parameters: $n = 0, K_0 = 1.2, a = 0.6, \gamma = 0.9, m = 0.9, d = 0.3$, and $\lambda = 0.3$, where the initial condition are taken at $(0.8, 0.9)$ and $(0.5, 0.5)$. The equilibrium solution $E = (0.3, 0.675)$ is stable.

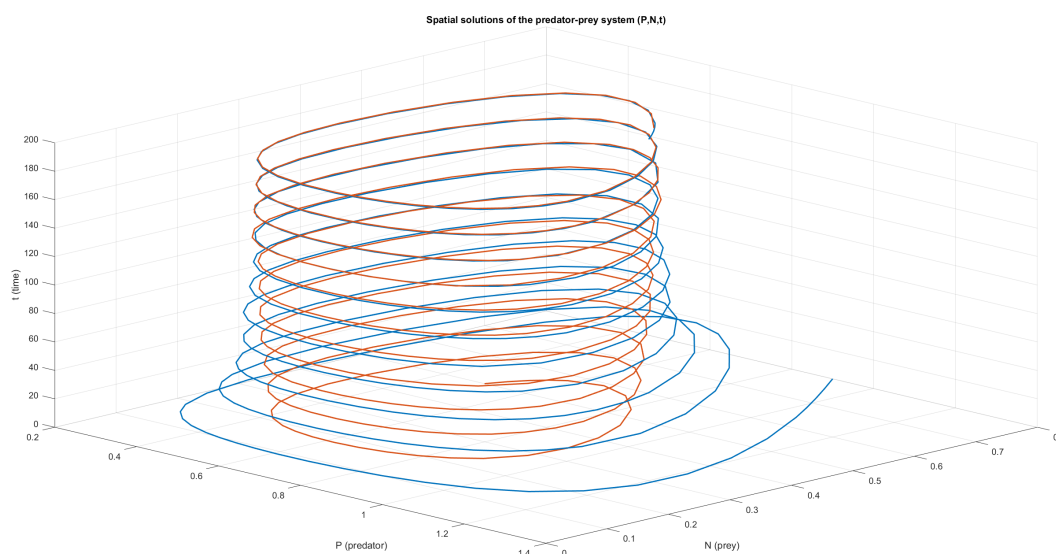


Figure 3. Numerical simulation for the ODE version of systems (1.1)–(1.2): $u(t)$; $v(t)$. We consider the following values of parameters: $n = 0$, $K = 1.3$, $a = 0.6$, $\gamma = 0.9$, $m = 0.9$, $d = 0.3$, $\lambda = 0.3$, where the initial condition are taken at $(0.8, 0.9)$ and $(0.5, 0.5)$. The equilibrium solution $E = (0.3, 0.692)$ is unstable and the solution converges to a spatially homogenous periodic orbit.

The corresponding ODE version of systems (1.1)–(1.2) involves parameters: γ , m , a , d , λ , and K . First, we choose parameters $\gamma = 0.9$, $m = 0.9$, $a = 0.6$, $d = 0.3$, and $\lambda = 0.3$. In this case, the Hopf bifurcation value is $K_0 = 1.2$. The equilibrium solution $E = (u_2, v_2)$ is locally asymptotically stable when $K < K_0$. At $K = K_0$, the equilibrium solution E loses the stability through a Hopf bifurcation. These are shown in Figures 1–3, where the initial condition are taken at $(0.8, 0.9)$ and $(0.5, 0.5)$.

On the other hand, our PDE models (3.11)–(3.12) involves parameters γ , m , a , d , λ , K , d_1 , and d_2 . One can choose the length parameter l so that several steady state bifurcation points occurs at K values bigger than K_0 . If $n = 1$, and we choose $\ell = 3.2$ with the values of parameters $d_1 = 0.5$, $d_2 = 0.5$, $a = 0.6$, $\gamma = 0.9$, $m = 0.9$, $\lambda = 0.3$, and $d = 0.3$, then we have $K_0 = 1.2$. In Figures 4–6, we illustrate the asymptotic behavior of the homogeneous solution of systems (3.11)–(3.12) for different values of K .

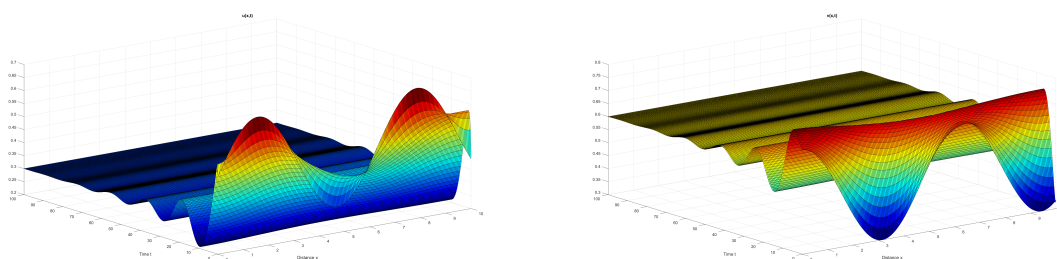


Figure 4. Numerical simulation of systems (3.11)–(3.12): (left) $u(x, t)$; (right) $v(x, t)$. We consider the following values of parameters: $n = 1$, $\ell = 3.2$, $K = 0.9$, $d_1 = 0.5$, $d_2 = 0.5$, $a = 0.6$, $\gamma = 0.9$, $m = 0.9$, and $d = 0.3$, where the initial condition is taken at $(u_0(x), v_0(x)) = (0.5 + 0.2 \sin(x), 0.5 + 0.2 \sin(x))$. The homogeneous equilibrium solution $E = (0.3, 0.6)$ is asymptotically stable.

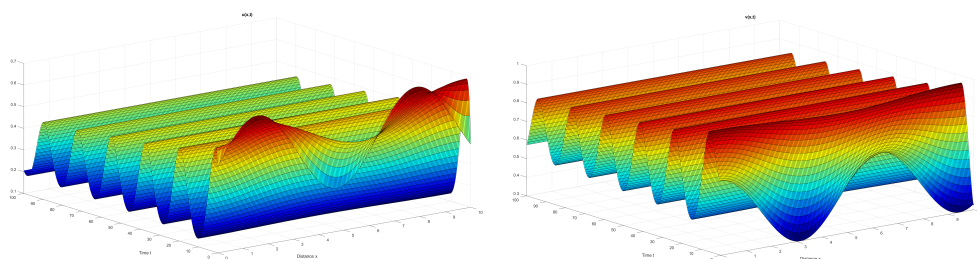


Figure 5. Numerical simulation of systems (3.11)–(3.12): (left) $u(x, t)$; (right) $v(x, t)$. We consider the following values of parameters: $n = 1$, $\ell = 3.2$, $K = 1.2$, $d_1 = 0.5$, $d_2 = 0.5$, $a = 0.6$, $\gamma = 0.9$, $m = 0.9$, and $d = 0.3$, where the initial condition is taken at $(u_0(x), v_0(x)) = (0.5 + 0.2 \sin(x), 0.5 + 0.2 \sin(x))$. The homogeneous equilibrium solution $E = (0.3, 0.675)$ is stable.

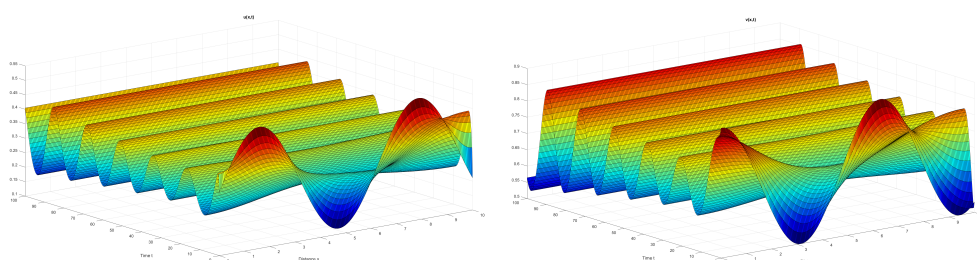


Figure 6. Numerical simulation of systems (3.11)–(3.12): (left) $u(x, t)$; (right) $v(x, t)$. We consider the following values of parameters: $n = 1$, $\ell = 3.2$, $K = 1.3$, $d_1 = 0.5$, $d_2 = 0.5$, $a = 0.6$, $\gamma = 0.9$, $m = 0.9$, and $d = 0.3$, where the initial condition is taken at $(u_0(x), v_0(x)) = (0.3 + 0.2 \sin(x), 0.7 + 0.2 \sin(x))$. The homogeneous equilibrium solution $E = (0.3, 0.692)$ is unstable and the solution converges to a spatially homogenous periodic orbit.

5. Conclusions and remarks

The most realistic population models are those that consider the effect of space on species dynamics, which requires the use of reaction-diffusion equations. These models describe how populations grow and evolve in one-, two-, or three-dimensional environments, incorporating both biological interactions and spatial processes. In this context, Hopf bifurcation plays a crucial role, as it determines the emergence of periodic oscillations in populations, influencing their long-term coexistence.

In Section 2, we analyze the general reaction-diffusion systems (2.1)–(2.3) under Neumann boundary conditions in the spatial domain $\Omega = (0; \ell\pi)$, with $\ell \in \mathbb{R}^+$. We apply the method developed in [8] to derive expressions for the first Lyapunov coefficient, enabling us to verify the non-degeneracy conditions for codimension 1 Hopf bifurcation. These results provide crucial insights into the emergence of periodic orbits and their spatial behavior, identifying how diffusion influences the stability of periodic solutions. Furthermore, the procedure used can be extended to compute higher-order Lyapunov coefficients, broadening the analysis of the system's dynamics.

As an application of this approach, we consider a model in which two predator species compete for the same prey. In the absence of predators, the prey follows logistic growth, while predation is modeled using a generalized Holling III functional response. In this scenario, one predator acts as a K -strategist and the other as an r -strategist, generating different coexistence patterns. In Section 3, we demonstrate that when one of the predators is absent, systems (3.1)–(3.2) undergoes a codimension 1 Hopf bifurcation, leading to the emergence of periodic solutions. Depending on the system's conditions, these solutions can be spatially homogeneous, coinciding with the dynamics described by the corresponding ODE model, or spatially non-homogeneous, giving rise to temporal oscillations or stationary spatial patterns. This result is key to understanding how diffusion and Hopf bifurcation can facilitate periodic species coexistence. From microbiological and ecological perspectives, these findings indicate that spatial heterogeneity and microbial dispersal can enhance microbial diversity by facilitating oscillatory coexistence, preventing competitive exclusion, and generating spatiotemporal niches where sensitive and resistant strains or species can persist. Notably, the coexistence of K and r strategist microbial populations in structured environments reflects patterns observed in real-world ecosystems, such as biofilms, soil communities, and the gut microbiome, where species with contrasting life history strategies partition space and resources. This spatial and functional differentiation reduces direct competition and contributes to overall ecosystem stability.

Researchers have analyzed the ODE version of systems (1.1)–(1.2) and obtained similar bifurcation results in [14, 26, 27]. However, our analysis confirms that diffusion does not fundamentally alter the qualitative behavior of the system but reinforces it, sustaining species coexistence even in heterogeneous environments.

This highlights the importance of spatial processes in microbial ecology and conservation, where the connectivity of microhabitats (such as pores in soil or niches in biofilms) can critically influence the persistence and resilience of microbial populations. Understanding how diffusion interacts with local dynamics provides valuable insights for designing interventions to maintain microbial diversity, control infections, or manage antibiotic resistance in natural and clinical settings. We emphasize that the cascade of Hopf and steady-state bifurcations described in this paper illustrates the complex self-organized spatiotemporal dynamics of diffusive ecological systems. Although we focus on the

three-dimensional restriction of the system of partial differential equations given by (1.1)–(1.2), the methods employed can be extended to higher-dimensional systems or those with more parameters, enabling a more detailed analysis of the role of diffusion in population stability and growth. Biologically, this suggests that higher-dimensional microbial habitats, such as polymicrobial biofilms or gut environments, may harbor even more intricate dynamic regimes where both spatial complexity and local interactions shape microbial persistence and fluctuations. Incorporating such complexity is essential to accurately predict microbial responses to environmental change, antibiotic treatments, or microbial invasions.

Finally, as mentioned in the introduction, the predator-prey model studied in this paper, which presents Hopf bifurcation and considers diffusion, is a powerful tool to study complex biological dynamics, such as those observed in pathology, immunology, and antimicrobial resistance. Our model in particular can be adapted to problems of tumor pathology, immunology, infections, and antimicrobial resistance where the prey can be considered tumor cells, pathogenic bacteria, and sensitive and resistant bacterial populations, and predators as immune cells, macrophages or antibiotics, antimicrobials, or phagocytes. This interdisciplinary applicability highlights the biological relevance of our findings, as they can inform medical strategies for controlling tumors, infections, or the evolution of resistance by leveraging oscillatory and spatially structured population dynamics. We defer our work in this direction to a subsequent exposition.

Use of AI tools declaration

The authors declare they have not used Artificial Intelligence (AI) tools in the creation of this article.

Acknowledgement

Jocirei D. Ferreira acknowledges the funding support from the Institute of Exact and Earth Science, Federal University of Mato Grosso, Barra do Garças, Brazil. Aida P. G. Nieva, Jhon J. Perez and Wilmer M. Yepez acknowledge support from the Departamento de Matemáticas, Universidad del Cauca, Popayán, Colombia.

Conflict of interest

The authors declare there is no conflict of interest.

References

1. W. W. Murdoch, C. J. Briggs, R. M. Nisbet, *Consumer-Resource Dynamics*, Princeton University Press, 2003.
2. R. S. Cantrell, C. Cosner, *Spatial Ecology via Reaction-Diffusion Equations*, Wiley, 2004.
3. G. Sun, J. Zhang, L. Song, Z. Jin, B. Li, Pattern formation of a spatial predator–prey system, *Appl. Math. Comput.*, **218**, (2012), 11151–11162. <https://doi.org/10.1016/j.amc.2012.04.071>
4. A. Okubo, *Diffusion and Ecological Problems: Mathematical Models*, Springer-Verlag, Berlin, 1981. <https://doi.org/10.1007/BF02851862>

5. D. Tilman, P. Kareiva, *Spatial Ecology: The Role of Space in Population Dynamics and Interspecific Interactions (MPB-30)*, Princeton University Press, USA, 1997.
6. J. Sotomayor, L. F. Mello, D. C. Braga, Lyapunov coefficients for degenerate Hopf bifurcations, preprint, arXiv:0709.3949.
7. D. D. Hassard, N. D. Kazarinoff, Y. H. Wan, *Theory and Application of Hopf Bifurcation*, *SIAM Rev.*, **24** (1982). <https://doi.org/10.1137/1024123>
8. F. Yi, J. Wei, J. Shi, Bifurcation and spatiotemporal patterns in a homogeneous diffusive predator-prey system, *J. Differ. Equations*, **246**, (2009), 1944–1977. <https://doi.org/10.1016/j.jde.2008.10.024>
9. J. D. Ferreira, A. González, W. Molina, Lyapunov coefficients for degenerate Hopf bifurcations and an application in a model of competing populations, *J. Math. Anal. Appl.*, **455** (2017), 1–51. <https://doi.org/10.1016/j.jmaa.2017.05.040>
10. J. Y. Wakano, K. Ikeda, T. Miki, M. Mimura, Effective dispersal rate is a function of habitat size and corridor shape: Mechanistic formulation of a two-patch compartment model for spatially continuous systems, *Oikos*, **120** (2011), 1712–1720. <https://doi.org/10.1111/j.1600-0706.2011.19074.x>
11. M. Cavani, M. Farkas, Bifurcations in a predator-prey model with memory and diffusion II: Turing bifurcation, *Acta Math. Hungar.*, **63** (1994), 375–393. <https://doi.org/10.1007/BF01874463>
12. M. Cristofol, L. Roques, Biological invasions: Deriving the regions at risk from partial measurements *Math. Biosci.*, **215** (2008), 158–166. <https://doi.org/10.1016/j.mbs.2008.07.004>
13. P. A. Hancock, H. C. J. Godfray Modeling the spread of Wolbachia in spatially heterogeneous environments, *J. R. Soc. Interface*, **76** (2012), 3045–3054. <https://doi.org/10.1098/rsif.2012.0253>
14. M. Farkas, Zip bifurcation in a competition model, *Nonlinear Anal. Theory Methods Appl.*, **8** (1984), 1295–1309. [https://doi.org/10.1016/0362-546X\(84\)90017-8](https://doi.org/10.1016/0362-546X(84)90017-8)
15. M. Farkas, *Periodic Motions*, Springer-Verlag, New York, 1994.
16. J. D. Ferreira, L. A. F. de Oliveira, Zip bifurcation in a competitive system with diffusion, *Differ. Equations Dyn. Syst.*, **17** (2009), 37–53. <https://doi.org/10.1007/s12591-009-0003-0>
17. M. Farkas, J. D. Ferreira, Zip bifurcation in a reaction-diffusion system, *Differ. Equations Dyn. Syst.*, **15** (2007), 169–183.
18. I. Szántó, Velcro bifurcation in competition models with generalized Holling functional response, *Appl. Math.*, **6** (2005), 185–195. <https://doi.org/10.18514/MMN.2005.115>
19. W. Ko, K. Ryu A qualitative study on general Gause-type predator-prey models with constant diffusion rates, *J. Math. Anal. Appl.*, **344** (2008), 217–230. <https://doi.org/10.1016/j.jmaa.2008.03.006>
20. J. Smoller, *Shock waves and Reaction-Diffusion Equations*, 2nd Edition, Springer-Verlag, New York, 1994.
21. Y. A. Kuznetsov, *Elements of applied Bifurcation theory*, Springer-Verlag, 1998.
22. A. Bazykin, A. Khibnik, B. Krauskopf, *Nonlinear Dynamics of Interacting Populations*, World Scientific, 1998. <https://doi.org/10.1142/2284>

23. H. Li, Y. Takeuchi, Dynamics of the density dependent predator-prey system with Bedington-DeAngelis functional response, *J. Math. Anal. Appl.*, **374** (2011), 644–654. <https://doi.org/10.1016/j.jmaa.2010.08.029>
24. S. Abbas, M. Banerjee, N. Hungerbuhler, Existence, uniqueness and stability analysis of allelopathic stimulatory phytoplankton model, *J. Math. Anal. Appl.*, **367** (2010), 249–259. <https://doi.org/10.1016/j.jmaa.2010.01.024>
25. S. Abbas, M. Sen, M. Banerjee, Almost periodic solution of a non-autonomous model of phytoplankton allelopathy, *Nonlinear Dyn.*, **67** (2012), 203–214. <https://doi.org/10.1007/s11071-011-9972-y>
26. E. Sáez, E. Stange, I. Szántó, Simultaneous zip bifurcation and limit cycles in three dimensional competition models, *SIAM J. Appl. Dyn. Syst.*, **5** (2006), 1–11. <https://doi.org/10.1137/040613998>
27. J. D. Ferreira, L. A. F. de Oliveira, Hopf and zip bifurcation in a specific $(n+1)$ -dimensional competitive system, *Mat. Enseñanza Univ.*, **15**, (2008), 35–41.



AIMS Press

© 2025 the Author(s), licensee AIMS Press. This is an open access article distributed under the terms of the Creative Commons Attribution License (<https://creativecommons.org/licenses/by/4.0>)